BIOREACTOR-MEDIATED GELATIN METHACRYLOYL MICROCARRIER EXPANSION AND HUMAN PLATELET LYSATE SUPPLEMENTATION: A SCALABLE MESENCHYMAL STEM CELL EXPANSION PLATFORM

A Dissertation

by

ROBERT EUGENE ROGERS

Submitted to the Graduate and Professional School of
Texas A&M University
in partial fulfillment of the requirements for the degree of

DOCTOR OF PHILOSOPHY

Chair of Committee,	Roland Kaunas
Committee Members,	Daniel Alge
	Carolyn Cannon
	Carl Gregory
Head of Department,	Carol Vargas-Bautista

May 2022

Major Subject: Medical Sciences

ABSTRACT

Bioreactor-mediated expansion of human mesenchymal stem cells (hMSCs) is a promising technique for the generation of hMSCs and their secreted products for immunoregulation therapies at scales required for use in the clinic. However, there are gaps in knowledge regarding how hMSCs behave on different microcarrier surfaces during bioreactor culture, and how the type of media supplementation alters their phenotype after expansion. The goals of the experiments presented in this dissertation were two-fold: 1) to characterize the behavior of a renewable source of induced pluripotent stem cell-derived mesenchymal stem cells (ihMSCs) in a scalable bioreactor platform using gelatin-based microcarriers generated with high-throughput microfluidics; and 2) to evaluate ihMSC phenotype in monolayer culture using xenogen-free media containing human platelet lysates (hPL).

Gelatin methacryloyl (GelMA) is a photocrosslinkable derivative of gelatin that has not previously been used for microcarrier-mediated bioreactor expansion of hMSCs for immunomodulatory applications. The immunomodulatory potency of the ihMSCs and their extracellular vesicles (EVs) were evaluated *in vitro*. The results demonstrate the ability to rapidly produce GelMA microcarriers using a step emulsification microfluidic device and their utility for the expansion of ihMSCs in a 100 mL vertical wheel bioreactor without compromising cell identity, while also enhancing the immunomodulatory potential of cells and harvested EVs. Additionally, the culture of these ihMSCs with hPL-supplemented media improved adipogenic differentiation

potential and EV production capabilities compared to ihMSCs culture in media supplemented with FBS while retaining their immunomodulatory potential.

DEDICATION

I would like to dedicate this dissertation to my family and to my wife, Dr. Josie Rossitto.

ACKNOWLEDGEMENTS

I would like to thank my committee chair, Dr. Kaunas, for the support, guidance, and mentorship he has given me throughout this research. I would also like to thank my committee members, Drs. Daniel Alge, Carolyn Cannon, and Carl Gregory, for their advice and assistance on this research and this project.

I also would like to thank the MD/PhD program staff for their support and assistance in my MD and PhD years. I also want to thank my colleagues for all their help and support during this research, especially my colleagues in the Kaunas lab including Robert Reese, Eli Mondragon, and Berkley White.

Finally, I want to thank my wife and my family for their support during my research.

CONTRIBUTORS AND FUNDING SOURCES

Contributors

This work was supervised by a dissertation committee consisting of Drs. Roland Kaunas and Daniel Alge of the Department of Biomedical Engineering, and Drs. Carolyn Cannon and Carl Gregory of the College of Medicine.

In Chapter 2, the fabrication of the silicon wafer microfluidic device templates was performed by Dr. Jing Dai of the Department of Electrical and Computer Engineering. The production of microcarriers was performed and analyzed in collaboration with Andrew Haskell and Berkley White of the College of Medicine and the Department of Biomedical Engineering, respectively. The degradation of microcarriers was evaluated in collaboration with Dr. Susan Woodard of the National Center for Therapeutics Manufacturing. The assays for immunophenotyping, clonogenicity, and trilineage differentiation potential were performed and analyzed in collaboration with Andrew Haskell, Berkley White, Dr. Ryang-Hwa Lee, and the College of Medicine Cell Analysis Facility. The data and analysis for exosome production and immunomodulation were performed by the laboratory of Dr. Ryang-Hwa Lee at the Institute for Regenerative Medicine.

In Chapter 3, the assays for trilineage differentiation potential were performed in collaboration with Berkley White. The data and analysis of trilineage differentiation potential were performed and analyzed in collaboration with Andrew Haskell and Berkley White. The assays for immunophenotyping, clonogenicity, and trilineage differentiation

potential were performed and analyzed in collaboration with Andrew Haskell, Berkley White, Dr. Ryang-Hwa Lee, and the College of Medicine Cell Analysis Facility. The data and analysis for exosome production and immunomodulation were performed by the laboratory of Dr. Ryang-Hwa Lee at the Institute for Regenerative Medicine.

All other work conducted for the dissertation was completed by the student independently.

Funding Sources

Graduate study was supported through a President's Excellence in Research Grant from Texas A&M University. Its contents are solely the responsibility of the authors and do not necessarily represent the official views of Texas A&M University.

NOMENCLATURE

ADM	Adipogenic Differentiation Medium
ALP	Alkaline Phosphatase
ANOVA	Analysis of Variance
ARS	Alizarin Red S
BM-hMSC	Bone Marrow-Derived Human Mesenchymal Stem Cells
CCM	Complete Culture Medium
CDM	Chondrogenic Differentiation Medium
CDPF	Chemically-Defined, Protein-Free
cGMP	Current Good Manufacturing Practice
COLI	Collagen I
DI	Deionized
DMEM	Dulbecco's Modified Eagle Medium
DNA	Deoxyribonucleic Acid
EDTA	Ethylenediaminetetraacetic Acid
ELISA	Enzyme-Linked Immunosorbent Assay
EV	Extracellular Vesicle
FABP4	Fatty Acid Binding Protein 4
FDA	Food and Drug Administration
GAPDH	Glyceraldehyde 3-Phosphate Dehydrogenase
GelMA	Gelatin Methacryloyl

hMSC	Human Mesenchymal Stem Cell
hPL	Human Platelet Lysate
IFN-γ	Interferon-γ
ihMSC	Induced Pluripotent Stem Cell-Derived Human Mesenchymal Stem Cell
IL-1β	Interleukin-1β
IL-10	Interleukin-10
IL-6	Interleukin-6
iPSC	Induced Pluripotent Stem Cell
ISCT	International Society of Cell & Gene Therapy
ITS	Insulin, Transferrin, Selenium
kDa	Kilodalton
kPa	Kilopascal
LAP	Lithium Phenyl-2,4,6-Trimethylbenzoylphosphinate
LPL	Lipoprotein Lipase
LPS	Lipopolysaccharide
MWCO	Molecular Weight Cutoff
NIH	National Institute of Health
OBM	Osteogenic Basal Medium
OBM+Dex	Osteogenic Basal Medium + Dexamethasone
OCN	Osteocalcin
ORO	Oil Red O
PBS	Phosphate-Buffered Saline

PDMS	Polydimethylsiloxane
PET	Polyethylene Terephthalate
PFA	Paraformaldehyde
PNPP	p-Nitrophenyl Phosphate
PPAR-γ	Peroxisome Proliferator-Activated Receptor-γ
qRT-PCR	Quantitative Reverse Transcriptase Polymerase Chain Reaction
RA	Rheumatoid Arthritis
RNA	Ribonucleic Acid
RPM	Rotations per Minute
RUNX2	Runt-Related Transcription Factor 2
RWVB	Rotating Wall Vessel Bioreactor
SDS	Sodium Dodecyl Sulfate
SLA	Stereolithography
SLE	Systemic Lupus Erythematosus
STC-1	Stanniocalcin-1
TGF-β1	Transforming Growth Factor-β1
TGF-β3	Transforming Growth Factor-β3
Th	Helper T-Cell
TNF-α	Tumor Necrosis Factor-α
T-Reg	Regulatory T-Cell
TSG-6	Tumor necrosis factor-inducible gene 6 protein

TABLE OF CONTENTS

Page

LIST OF FIGURES

Page

LIST OF TABLES

Page

CHAPTER 1

INTRODUCTION

1.1 Clinical Trials and Production of Human Mesenchymal Stem Cells (hMSCs)

1.1.1 Graft-Versus-Host Disease (GvHD) Treatment: A Success in hMSC Therapeutics

Acute GvHD (aGvHD) is a life-threatening complication that affects approximately 35-50% of allogeneic hematopoietic stem cell transplant recipients.[1] Pro-inflammatory cytokine release post-transplant triggers donor T-cells to mount an immune response against recipient tissues, leading to disorders of the gastrointestinal tract, liver, and skin. High-dose steroids are used to treat aGvHD, though the response rate of patients to therapy is only 30-50%.[2] There exists no standard protocol for treating steroid-resistant aGvHD (SR-aGvHD), and the five-year survival of patients with severe disease is only 25%.[3]

hMSCs have been studied as a therapeutic agent for SR-aGvHD due to their anti-inflammatory properties.[2,4,5] Though response to hMSC therapy varies depending on symptoms and disease severity, a recent collection of clinical trials reported success treating pediatric SR-aGvHD with intravenous allogeneic hMSC preparations (Ryoncil™), with 66% of patients responding to treatment. Of the responders, 83% survived 180 days after treatment.[6] In September 2020, Ryoncil™ is scheduled to be the first FDA-approved hMSC therapeutic with the potential to save thousands of lives per year.

Additional clinical trials have demonstrated that hMSCs or extraceullular vesicles (EVs) isolated from hMSCs are effective in treating the symptoms of

autoimmune diseases such as inflammatory bowel disease (IBD), rheumatoid arthritis (RA), and systemic lupus erythematosus (SLE), further reinforcing the potential application of hMSCs as anti-inflamatory therapeutics.[7-9]

1.1.2 Reducing Costs Through Donor and Stem Cell Source

The increasing number of clinical trials has led to high demand for hMSCs, with over 7 trillion cells needed in 2016 and 100 trillion cells needed for 2040 (Figure 1-1-A).[10] While it may be ideal to treat patients with autologous hMSCs to minimize risks of immune response, cells from patients with diseases such as SLE are senescent and lack immunosuppressive capabilities.[11] Additionally, allogeneic hMSCs can be expanded to larger batch sizes for treating multiple patients, reducing quality control steps and production costs by 66% compared to autologous therapy.[12]

The source for stem cell isolation is also important to consider for minimizing harm to the donor. hMSCs from bone marrow aspiration (BM-hMSCs) or lipoaspirates can lead to chronic pain and post-procedure complications. Umbilical cord-derived mesenchymal stem cells can be harvested without a loss, but still suffer from expansion limitations and donor-to-donor variability. ihMSCs can potentially circumvent complications and donor variability by producing MSC-like cells from a self-propogating iPSC line.[13] Additionally, previous studies have shown that ihMSCs can expand for 64 population doublings before reaching senescence, increasing the number of active cells at harvest compared to other tissue-derived hMSCs (Figure 1-1 B).[13,14]

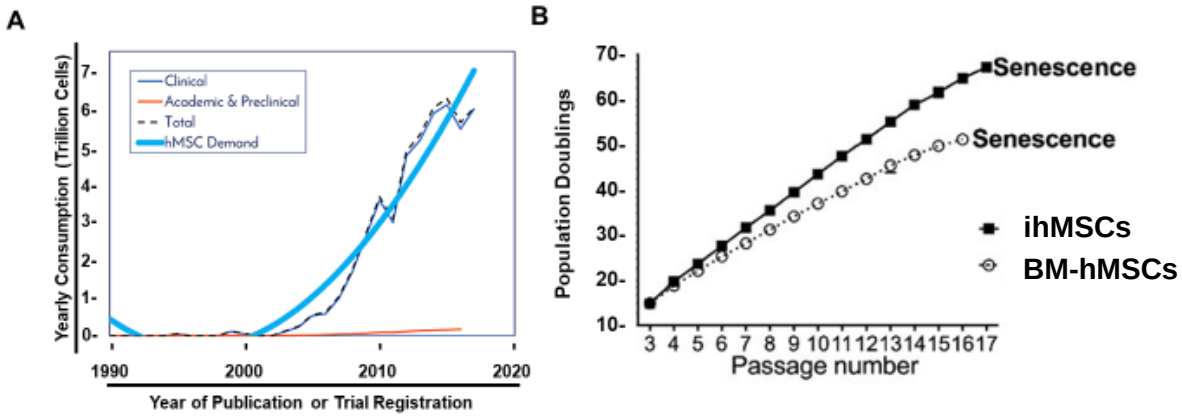

Figure 1-1: Historical hMSC Demand and Meeting Demand with ihMSC Expansion.
(A) hMSC demand since 2000 has risen to 7 trillion cells by 2016. Reprinted from [10].
(B) ihMSCs expand to higher cell numbers compared to BM-hMSCs. Reprinted from [13].

1.1.3 Optimum Reactor Design for hMSC Expansion

Previous studies have found that hMSC production costs are directly dependent on cell expansion potential, particularly the time between population doublings and the number of cells that can be isolated from a single culture vessel. Four types of bioreactors have been typically used for hMSC expansion: multilayer flasks (MLF), multiplate reactors (MPB), hollow-fiber bioreactors (HFB), and microcarrier-mediated bioreactors (STR).[15,16] Previous studies have identified MPB and STR expansion as the most cost-efficient techniques for generating large batches of allogeneic hMSCs (Figure 1-2 A). However, the maximum expansion area in STRs can exceed 11 million cm^2 per reactor, 100-fold higher than MPBs.[16] Additionally, hMSC expansion using xeno-free media reduces population doubling times compared to fetal bovine serum (FBS)-containing media, further reducing production costs by up to 16% (Figure 1-2 B).[10,16,17] By combining STR expansion and xeno-free media, production costs can be reduced to

the point where hMSC therapeutics are competitive with currently-approved therapeutics.[6]

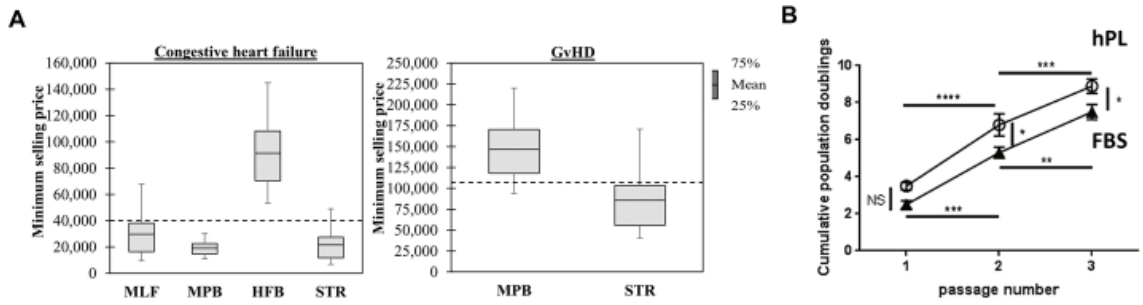

Figure 1-2: Techniques to Reduce hMSC Production Costs.
(A) Economic modeling of hMSC expansion demonstrates that MPB and STR bioreactors are the only two technologies capable of generating hMSC doses that are below the current insurance reimbursement rates for congestive heart failure and GvHD. Reprinted from [16]. (B) hMSC expansion in hPL compared to FBS increases the number of population doublings over three passages. Reprinted from [18].

1.2 hMSCs: Origin and Immune Modulation Mechanisms

1.2.1 Defining hMSCs and Immunomodulatory Mechanisms

Human mesenchymal stem cells were originally identified as colony-forming fibroblastic cells that were collected from the bone marrow and were responsive to irradiation.[19] Further research into these cells identified that they could self-renew, expressed a specific set of cellular surface markers, and were capable of differentiating along adipo-, chondro-, and osteogenic lineages. These were eventually employed in 2006 as the minimal criterion for defining and identifying hMSCs.[20]

Subsequent research has led to the discovery that hMSCs can alter the immune system through several different mechanisms. Pro-inflammatory cytokines such as Interferon-γ (IFN-γ), Tumor Necrosis Factor-α (TNF-α), and Interleukin-1β (IL-1β) prime hMSCs to produce and support an anti-inflammatory environment through

stimulation of regulatory T-cell expansion, suppression of Th1, Th2, and Th17 cells, and induction of anti-inflammatory antigen presenting cells, including anti-inflammatory M2 macrophages.[21] The anti-inflammatory mechanisms of hMSCs occur through the secretion of soluble factors, direct cellular interactions, and the release of extracellular vesicles (EVs) (Figure 1-3).

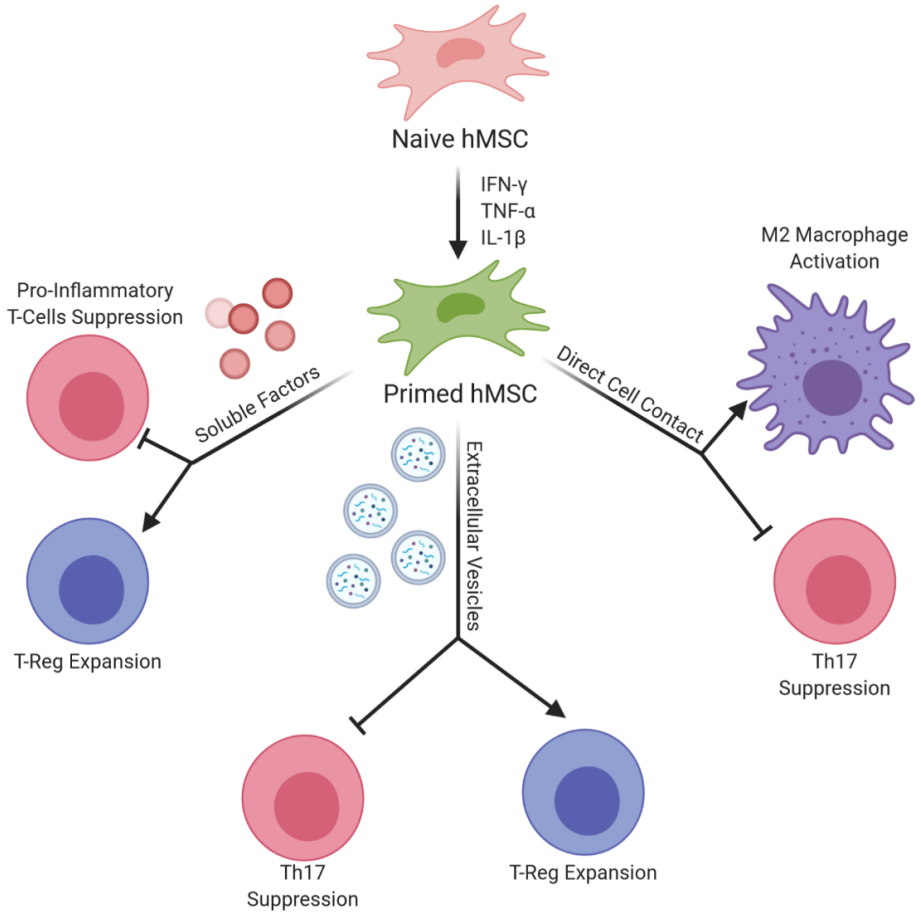

Figure 1-3: The Various Mechanisms by Which MSCs Exert Their Effect on the Immune System.
After being primed with cytokines such as IFN-γ, TNF-α, and IL-1β, hMSCs can cause immunomodulation via a number of mechanisms including soluble factor release, cell-cell interactions, and the release of EVs. The broad effects are to inhibit the expansion of pro-inflammatory cell types while driving the activation and expansion of anti-inflammatory cells such as T regulatory lymphocytes (T-Regs) and M2 macrophages. Adapted from [21].

1.2.2 EVs and their Properties

EVs have attracted interest as a cell-free therapeutic because they can be isolated from cell culture media and can suppress inflammatory responses. In particular, they have been shown to inhibit pro-inflammatory T-cell proliferation, particularly Th17 cells. At the same time, they induce T-Reg proliferation and IL-10 secretion.[21]

There are three types of EVs, each being produced via different mechanisms and affecting the immune system in different ways.[22-24] Exosomes are particles 30-150 nm in diameter that are derived from endosomes and are stored in multivesicular bodies. Exosomes are released during fusion of multivesicular bodies with the plasma membrane. They contain a number of biological materials including mitochondria, RNA, proteins, and signaling molecules.

Upon arrival at their target destination, exosomes are endocytosed and either interact directly with membrane bound receptors or fuse with another intracellular lipid bilayer, releasing their contents into the cytoplasm. Key mediators of exosome effects on immunomodulation include Transforming Growth Factor- β1 (TGF-β1), Pentraxin-Related Protein (PTX), and micro-RNAs let7b and mir-21.[25] Microvesicles (150-600 nm diameter) and apoptotic bodies (>1000 nm diameter) are also part of the EV family, but are usually produced during cellular stress responses and are formed directly from the plasma membrane.

1.2.3 Generating EVs

The production of EVs derived from hMSCs or hMSC-secreted exosomes requires large surface areas to generate relevant therapeutic quantities of either

material.[26,27] In addition to being able to generate higher cell densities than traditional monolayer culture, microcarriers can aggregate into three dimensional structures during culture, improving the immunomodulatory potential of the expanding hMSCs through an unknown mechanism.[28,29] Previous studies have reported increased gene expression of TNFα stimulated gene/protein 6 (TSG-6) and other anti-inflammatory proteins in hMSCs aggregated in spheroids and cultured on microcarrier surfaces in bioreactors compared to hMSCs cultured in monolayer.[25,28] TSG-6 exerts its effect on macrophages, changing them from a proinflammatory (M1) to an anti-inflammatory (M2) phenotype. Therefore, the identification of materials or culture conditions that can improve immunomodulatory potential during microcarrier expansion are key to the development of cell therapeutics.

1.3 Microfluidic Devices for Custom Microcarrier Preparations

1.3.1 Properties of Microcarrier and Gelatin Methacryloyl (GelMA)

Commercially available microcarriers are prepared from a number of materials and coatings, depending on the desired application.[30] Most commercially available microcarriers are non-degradable, necessitating separation technologies such as tangential flow filtration to isolate cellular product.[31] Degradable, naturally-derived materials have been explored for hMSC expansion to remove the need for filtration and separation.[32] In particular, gelatin-based materials have integrin binding domains and can be crosslinked using several strategies.[33,34] A derivative of gelatin, GelMA, is a promising material due to the ease of fabrication and tunability of the resulting mechanical properties.[35] GelMA is often produced by the reaction of gelatin with

methacrylic anhydride, resulting in methacryl group addition to amino acids with primary amines or hydroxyls (Figure 1-4).[36] The methacryl groups will react via radical-mediated polymerization to form a covalent network between gelatin molecules. The bloom strength, extraction technique, degree of functionalization, and weight percentage of gelatin in the prepolymer solution directly affect mechanical and chemical properties including stiffness, integrin binding site density, and prepolymer viscosity.[37]

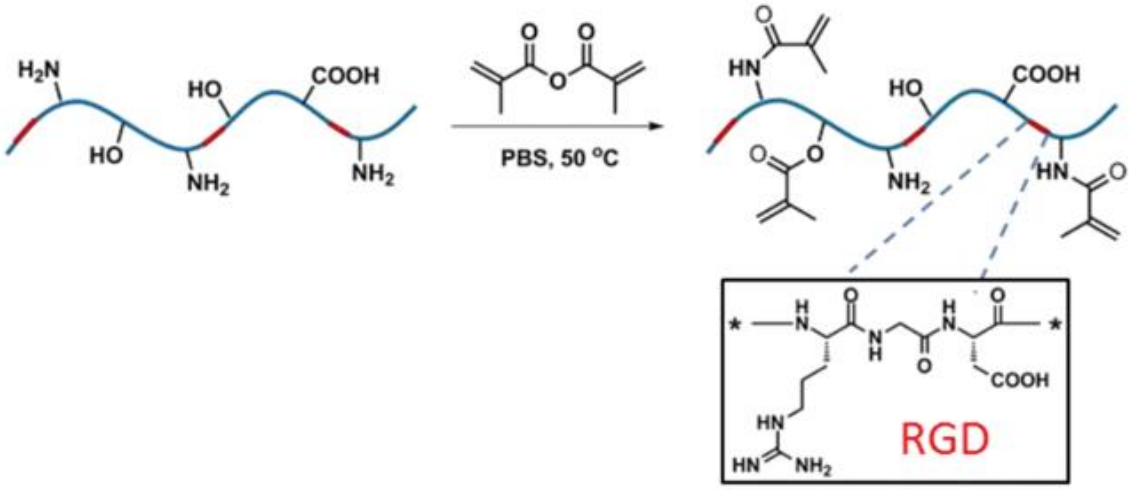

Figure 1-4: GelMA Reaction Overview and Integrin Binding Potential
The overall reaction schematic for GelMA production whereby methacrylic anhydride covalently modifies primary amines and hydroxyls on the gelatin molecule (blue). These methacryl groups can be covalently-crosslinked using radical mediated polymerization. However, integrin binding sites are such as RGD (Red) are preserved after metacryl addition and polymerization. Reprinted from [**35**].

1.3.2 Generating GelMA Microcarriers

The generation of microcarriers from GelMA typically is performed using water-in-oil emulsion techniques, where the aqueous GelMA prepolymer solution is broken into small droplets in an organic or insoluble fluid and kept separated using surfactants before polymerization. After polymerization, the GelMA microcarriers are purified and

used in their desired applications.[38-41] A number of techniques can be used to generate GelMA microcarriers, from mechanical disruption via vortexing to electrospray of the prepolymer solution into oil.[42,43] However, microfluidic techniques are a more reliable method of generating microcarriers with specific diameters and low polydispersity.[44]

Of the different droplet formation mechanisms, step emulsification has emerged as a candidate for high throughput generation of microcarriers because of the relative independence of droplet formation and inlet flowrates, in contrast to flow-focusing microfluidic devices.[45,46] The formation of droplets begins by the introduction of a fluid into a channel that steps into a larger space filled with immiscible fluid. The curvature of the forming droplet causes a pressure difference to form between opposite ends of the droplet, where the inlet fluid begins to form a "neck" of fluid. As the droplet continues to form, the pressure drop between the droplet and neck decreases, driving fluid into the forming microcarrier. At a critical pressure difference, the fluid flowing from the neck into the droplet exceeds the fluid flowing from the remaining prepolymer solution into the neck, leading to the neck decreasing in size until it detaches from the nozzle, collapsing due to Rayleigh-Plateau instability (Figure 1-5).

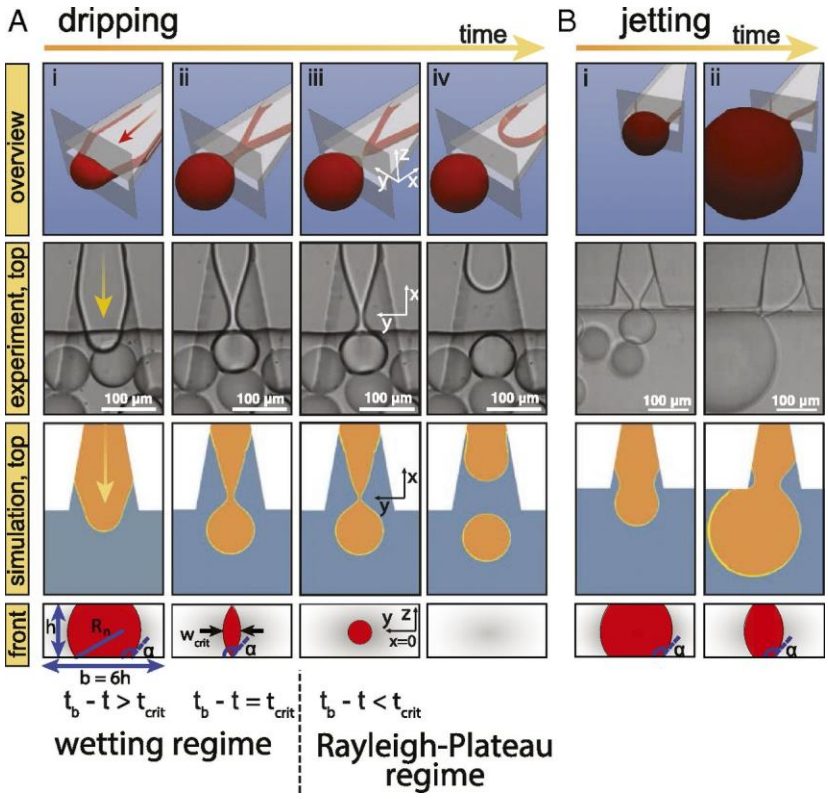

Figure 1-5: Mechanism of Droplet Production Using Step Emulsification
In this figure, the production mechanisms of droplet formation in the dripping (left) and jetting (right) regimes are shown from several views, including from the view of the neck in the bottom panel. Reprinted from [46].

This mechanism of microcarrier fabrication is primarily dependent on the prepolymer viscosity and the interactions between the prepolymer solution and the material that forms the neck.[46] There is a critical flowrate that, if exceeded, prevents the collapse of the neck before the formation of the next droplet. Droplet generation at flowrates exceeding the critical flowrate occurs via jetting and leads to higher droplet diameter and size dispersity. Several models have been developed to predict the critical flowrate for step emulsification devices using the capillary number, a ratio of viscous

forces of the dispersed fluid to the surface tension between the dispersed and continuous phases.[46,47]

One advantage of step emulsification is the linear scalability of droplet formation, as the critical flowrate scales linearly with the number of step channels on the device. Additionally, the features of step emulsification microfluidic devices permit their fabrication using polydimethylsiloxane (PDMS) molds of a silicon wafer mask prepared using soft photolithography.

1.4 Xeno-free hMSC Culture Using hPL

1.4.1 Benefits and Molecular Mechanisms of hPL Supplementation

As knowledge about hMSCs grows, quality criteria have been developed to minimize the risk of adverse events. The FDA has released guidelines recommending the elimination or minimization of animal products in cell-therapy production.[48-52] hPL has emerged as an allogeneic alternative for hMSC expansion that is affordable to both manufacture and purchase.[53] hPL offers several advantages over FBS for hMSC expansion including decreased immunoreactivity.[53-55] Platelet units can also be combined in large numbers to minimize lot variability, with a previous study showing that pooling of more than 200 platelet units per batch decreases variability in composition and cell behavior.[27,51,54-56]

A number of proteins and materials that contribute to the expansion-promoting effects of hPL are found in the alpha granules of intact platelets (Figure 1-6). Through lysis mechanisms including freeze/thaw cycles, platelet activation with exogenous materials, or mechanical disruption, alpha granules release material into the surrounding

plasma, increasing the concentration of growth factors to levels suitable for hMSC expansion.[56]

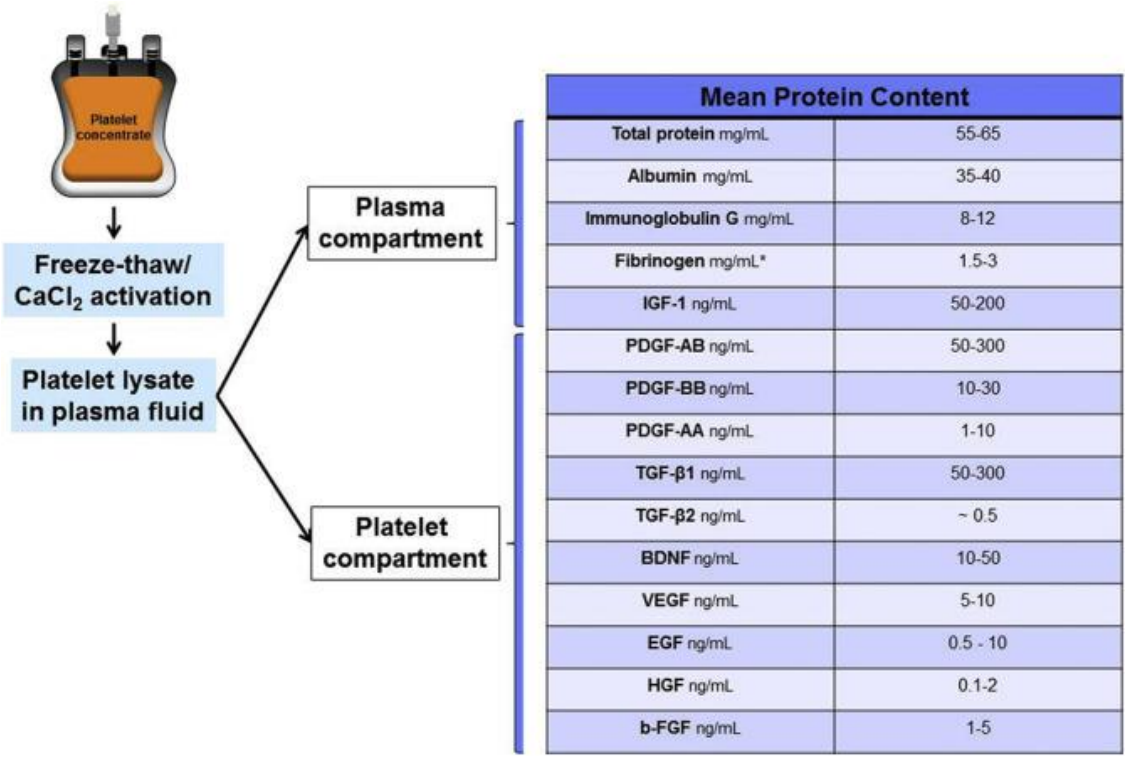

Mean Protein Content	
Total protein mg/mL	55-65
Albumin mg/mL	35-40
Immunoglobulin G mg/mL	8-12
Fibrinogen mg/mL*	1.5-3
IGF-1 ng/mL	50-200
PDGF-AB ng/mL	50-300
PDGF-BB ng/mL	10-30
PDGF-AA ng/mL	1-10
TGF-β1 ng/mL	50-300
TGF-β2 ng/mL	~ 0.5
BDNF ng/mL	10-50
VEGF ng/mL	5-10
EGF ng/mL	0.5 - 10
HGF ng/mL	0.1-2
b-FGF ng/mL	1-5

Figure 1-6: Platelet Components Recovered in hPL
A number of the growth factors and proteins are present in both hPL and FBS, with important components derived from both plasma and platelet alpha-granules.[57,58] Reprinted from [58].

1.4.2 Preparing hPL for Use in Cell Culture

A number of studies characterizing the effect of hPL supplementation have found that it supports improved expansion of hMSCs from various tissue sources compared with FBS.[49,59] In addition, several studies have found that hPL improves the osteogenic differentiation potential of hMSCs.[60,61] However, early studies used heparin to prevent fibrinogen polymerization in the culture media. The fibrinogen in hPL bound to hMSCs, limited their ability to inhibit T-cell proliferation, and increased their immunogenicity.[62]

To address this issue, fibrinogen can be removed from hPL by treatment with calcium to stimulate the coagulation cascade and form a fibrin polymer network.[63] Mechanical disruption of the fibrin network allows for recovery of the platelet lysate and reduction of fibrinogen by three orders of magnitude, though the concentration of some growth factors is reduced due to interactions with the polymerized fibrin.[63] Fibrinogen-reduced human platelet lysate has been shown to remove the requirement for porcine-derived heparin in culture media, further assisting the transition to xeno-free cell culture.

There are concerns about the use of human platelet lysates due to the poorly understood characteristics of the generated material.[55] Critical quality attributes are still being determined, and the possibility of transmitting infectious diseases remains a concern. However, techniques such as electron beam irradiation of the platelet lysate product, pooling of hundreds if not thousands of platelet donations, and current good manufacturing practice (cGMP)-compliant production and validation can reduce or mitigate the risks for hMSC production.[51,54,64]

1.5 Dissertation Overview and Approaches

1.5.1 Section 2: Bioreactor Expansion of ihMSCs on GelMA Microcarriers

In this section, GelMA microcarriers were prepared using several different types of microfluidic devices and eventually mass-produced using a step emulsification microfluidic device. These microcarriers were used to expand ihMSCs in well plates, rotating wall vessel bioreactors (RWVBs) and vertical wheel bioreactors. Cell identity was determined using colony forming unit assays, morphologic evaluations, and trilineage differentiation potential. EVs were harvested from and quantified from the

vertical wheel bioreactor. Finally, the ihMSCs and EVs were assayed for immunomodulatory potential using an *in vitro* splenocyte activation assay.

1.5.2 Section 3: Culture of ihMSCs in hPL

In this section, ihMSCs were cultured in culture medium containing hPL or FBS. Population doubling times and colony forming unit assays were used to determine the concentration of platelet lysate to use for media supplementation. Morphologic differences between cells cultured in hPL or FBS were quantified using CellProfiler®. Trilineage differentiation and immunomodulatory potential was also evaluated in cells cultured in both supplements. Finally, EV production capabilities and immunomodulatory potential were determined after ihMSC expansion in either FBS or hPL.

CHAPTER 2

ANALYSIS OF HUMAN MESENCHYMAL STEM CELLS AFTER BIOREACTOR-MEDIATED EXPANSION ON DEGRADABLE GELATIN METHACRYLOYL MICROCARRIERS

2.1 Introduction

hMSCs and their secreted products have been found to be effective in treating disorders resulting from a heightened immune response, demonstrated by several clinical trials and preclinical studies.[65-67] In particular, hMSCs and hMSC-derived EVs have been used successfully to treat GvHD, RA, and perianal fistulas of Crohn's disease in humans .[7-9,67,68] To meet the expected future demand for hMSC and hMSC-derived EV therapy, there is a pressing need to develop scalable methods for hMSC and EV production while retaining immunomodulatory function.[10,12,69]

Current methods for production of hMSCs and hMSC-derived EVs are largely reliant on monolayer culture techniques. However, hMSC expansion on microcarriers in STRs is a more efficient, scalable, and cost effective technique to produce the billions of cells necessary for therapeutic lot production.[70-72] Microcarrier expansion does not compromise stem cell identity or potency, and has even been found to improve the effectiveness of harvested EVs for immunomodulatory applications.[73,25,74]

Commercially available microcarriers have diverse characteristics that impact the ability to expand and recover hMSCs.[75,76] Polystyrene-based microcarriers have the advantage of robust mechanical properties but are non-degradable, requiring filtration to remove the hMSCs and EVs following production.[31] Degradable microcarriers, such as

gelatin-based microcarriers, improve the recovery of cells circumventing the need for filtration.[77] However, gelatin-based commercially available microcarriers are porous, which allows for invasion of the hMSCs into the microcarrier during culture, resulting in apoptosis of the cells at the core of these microcarriers and reducing recovery.[78]

Combining a non-porous, biodegradable microcarrier with scalable bioreactor technologies could provide a platform for improved isolation of hMSCs and EVs. GelMA is a photo-crosslinkable derivative of gelatin that retains integrin-binding and enzymatic-degradation potential while forming covalent crosslinks between gelatin molecules.[39,79] Microcarriers prepared from GelMA have previously been used for the expansion of hMSCs on low attachment well plates without penetration of hMSCs into the microcarrier.[39] However, GelMA microcarriers have not been used for the expansion of hMSCs in scalable bioreactors. Additionally, they have not been used for the production of hMSCs or EVs for immunomodulatory applications.

It is necessary to not only optimize bioreactor and microcarrier platforms, but also to select the appropriate donor for cell expansion. ihMSCs can be prepared from a single stock of iPSCs, permitting the production of trillions of cells with identical properties from a single donor.[13,14] The immunomodulatory capabilities of ihMSCs and ihMSC-derived EVs are comparable to those from BM-hMSCs both *in vitro* and in preclinical models of inflammatory diseases.[80] However, the expansion of ihMSCs in scalable bioreactor technologies has not been reported.

In this study, we hypothesized that GelMA microcarriers produced using a step emulsification microfluidic device can serve as a degradable microcarrier platform for

the expansion of ihMSCs in scalable bioreactors without compromising stem cell identity or immunomodulatory capabilities. To test this hypothesis, ihMSCs were expanded on GelMA microcarriers in vertical wheel or RWVBs and evaluated based on their stem cell identity and immunomodulatory potential. We also hypothesized that extracellular vesicles produced from ihMSCs following microcarrier expansion would retain immunomodulatory potential. We compared the results of our fabricated GelMA microcarriers with a commercially available collagen-coated polystyrene microcarrier (Pall-Solohill) that has previously been used for hMSC expansion in bioreactors.[75,81,82]

2.2 Methods

2.2.1 GelMA Synthesis and Characterization

GelMA was synthesized after modifications were made to a protocol by Loessner et al.[83] Briefly, type A porcine gelatin, bloom 300 (Sigma) was reacted with methacrylic anhydride (0.6 mL methacrylic anhydride/g gelatin) in phosphate-buffered saline (PBS) for 1 hour at 50 ^{o}C with vigorous stirring. After quenching the reaction with 40 ^{o}C PBS and dialyzing for 7 days through a 12-14 kDa nitrocellulose membrane against deionized water at 40 ^{o}C, the pH was readjusted to 7.4 using 1 M sodium bicarbonate ($NaHCO_3$), filtered through a 0.2 μm polyethersulfone (PES) filter, and lyophilized for 7 days in 0.2 μm filtered conical tubes. The number of functionalized amines was determined using a fluorescamine reagent according to the manufacturer's protocol (Thermo-Fisher). Viscosity at 40 ^{o}C was measured over 1 min using rheology at a constant strain of 1/s (MCR 301 Rheometer, Anton Paar).

2.2.2 Compressive Mechanical Testing of Crosslinked GelMA

Elastic modulus of bulk GelMA hydrogels were measured using dynamic mechanical analysis at 37 ^{o}C using a stress-strain sweep at a rate of 5% strain/min for 3 min (Q800, TA Instruments). The elastic modulus of individual microcarriers was estimated from the force-displacement relationship with a microcantilever with a flat indenter (Figure 2-1).

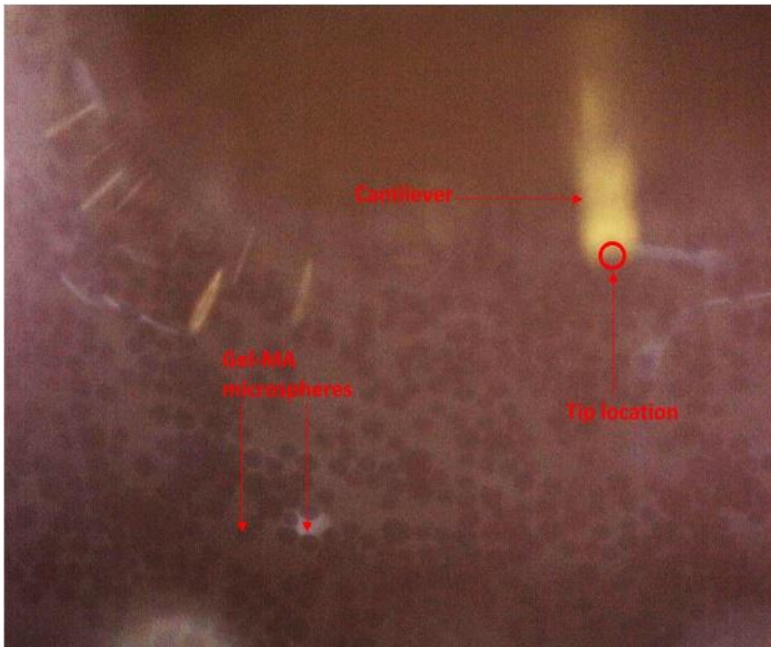

Figure 2-1: Nanoindentation Analysis for Determining GelMA Microcarrier Elastic Modulus
Micrograph of nanoindentation to measure the GelMA microsphere force-displacement curve. Microcarriers stained with Trypan Blue were tethered to the bottom surface of a polystyrene plate using EDC-NHS chemistry and kept hydrated in PBS buffer until measurement. The nanoindenter cantilever, cantilever tip, and individual GelMA microcarriers are indicated.

2.2.2 Microfluidic Step Emulsification Device Fabrication

A master mold for the microfluidic device was developed on a silicon wafer with SU-8™ 2025 (20 µm height) and 2075 photoresist (180 µm height, Microchem Inc.) using conventional soft photolithography. PDMS (10:1 mixture, Sylgard 184) was

poured over the master mold and polymerized at 85 ^{o}C for 1 hour. PDMS components and a 2” x 3” glass slide were exposed to 1 minute of oxygen plasma treatment, pressed together to form a covalent bond, and cured overnight at 85 ^{o}C. The assembled microfluidic device was then treated with Aquapel™ (3M) to make the microfluidic surface fluorophilic and sterilized by autoclaving prior to microcarrier production.

2.2.3 GelMA Microcarrier Fabrication

Two techniques were used to manufacture GelMA microcarriers, an SLA-printed coaxial flow-focusing device and a 100-channel step emulsification microfluidic device (Figure 2-2). Microcarriers were generated and purified in a biosafety cabinet to maintain sterile conditions. Microcarrier production rates, oil consumption rates, and diameter distributions were used to determine the optimal technique for microcarrier generation in subsequent experiments.

To produce microcarriers with the coaxial flow device, GelMA and photoinitiator lithium phenyl-2,4,6-trimethylbenzoylphosphinate (LAP) were dissolved in PBS at 50 ^{o}C to a final concentrations of 7.5% (w/v) and 1% (w/v), respectively.[84] The GelMA solution and mineral oil (Light Mineral Oil with 1% (v/v) Span-80, Sigma) were added to syringes and connected to the microfluidic device using Tygon™ ABW00001 tubing. Peristaltic pumps were used to perfuse the device with GelMA and mineral oil at flow rates of 0.6 mL/hr and 15 mL/hr, respectively. Microcarriers were then exposed to 365 nm-wavelength ultraviolet light (120 mW/cm^2) for 2 minutes before collection into a beaker filled with ice water. The microcarrier and water mixture was decanted into 50 mL conical tubes, and the microcarriers were separated from residual oil using

centrifugation at 1650 xg for 10 min. Microcarriers were washed three times with PBS before storage in PBS at 4 ^{o}C.

To produce microcarriers with the step emulsification device, GelMA and LAP were dissolved in PBS at 50 ^{o}C to final concentrations of 4% or 7.5% (w/v) and 10 mM, respectively. The GelMA solution and fluorinated oil (Novec 7500 with 1% (v/v) PicoSurf-1, Sphere Fluidics) were added to syringes and connected to the microfluidic device using Tygon™ ND 100-80 tubing (0.01" ID x 0.03" OD, Saint Gobain). Peristaltic pumps were used to perfuse the device with GelMA and fluorinated oil at 2 mL/hr and 4 mL/hr, respectively, for microcarrier generation. Microcarriers and fluorinated oil flowed into Tygon ND 100-80 tubing (0.02" ID x 0.06" OD, Saint Gobain) and were exposed to 365 nm-wavelength ultraviolet light (75 mW/cm^2) for 50 seconds before collection into a 50 mL conical tube. After removing the majority of fluorinated oil by pipet, the microcarriers were separated from the residual oil by centrifugation over a 20 mL glycerol bed at 3,000 xg for 60 seconds. Microcarriers were transferred to another 50 mL conical tube through a 300 µm strainer, washed three times using PBS, and stored at 4 ^{o}C until use.

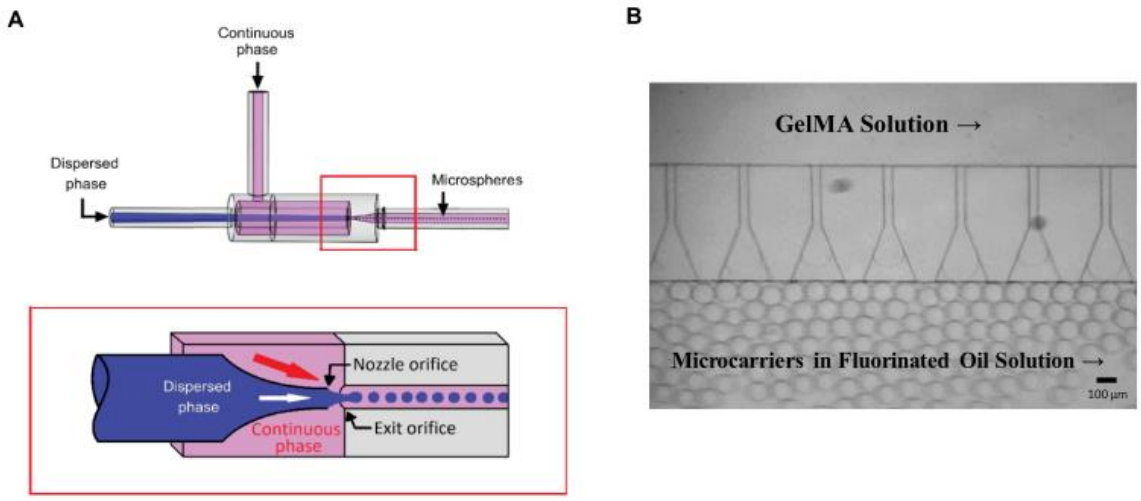

Figure 2-2: Coaxial Flow and Step Emulsification Microfluidic Devices Used in This Study
(A) A representative image of the coaxial flow microfluidic device is shown, along with a magnified image of the nozzle shown below. (B) A representative image of the step emulsification microfluidic device in generating GelMA microcarriers. Scale Bar represents 100 µm. Images from (A) were adapted from [85].

2.2.4 Quantifying Microcarrier Diameter

Images of microcarriers were acquired using bright field microscopy during and after purification. The diameters were quantified using a custom Matlab™ (Mathworks) code. Histograms and plots of diameters during production were generated using Prism™ (GraphPad).

2.2.5 Monolayer Cell Culture

Induced pluripotent stem cell-derived human mesenchymal stem cell (ihMSCs) were provided by Dr. Carl Gregory and prepared as previously described.[13] Cells were seeded at 500 cells per cm^2 on tissue culture polystyrene and expanded in complete culture medium (CCM) containing α-Minimum Essential Media (Invitrogen), 10% (v/v) Fetal Bovine Serum (FBS, Atlas Biologicals), 4 mM L-Glutamine, and 100 U/mL

penicillin and streptomycin changed every 2-3 days. Upon reaching 70% confluence, cells were exposed to 0.25% trypsin, 0.1% EDTA (Corning) at 37 ^{o}C for 5 minutes. After deactivating trypsin with CCM, cells were collected by centrifugation at 500 xg for 5 minutes. ihMSCs from passage 3-6 were used for experiments.

2.2.6 Microcarrier Degradation Assay

To optimize degradation methods, 4% GelMA microcarriers were placed in CCM and incubated overnight to allow for serum protein attachment. This incubation step was used in subsequent microcarrier experiments listed below. After the overnight incubation, 5 cm^2 of microcarriers were placed into 1.7 mL Eppendorf tubes and washed twice with 1X PBS. The microcarriers were then exposed to 1 mL of 0.25% trypsin, 0.1% EDTA (Corning), 0.05% TrypZEAN™, or Accutase™ and were incubated with agitation at 37 ^{o}C for 5 minutes, conditions used for ihMSC release from microcarrier and monolayer surfaces. Afterwards, microcarrier mixtures were transferred to wells of a 12-well plate containing 1 mL CCM and imaged using phase-contrast microscopy to assess the degree of degradation.

2.2.7 Microcarrier Attachment Assay

ihMSCs were added for a final seeding density of 1,000, 5,000, or 10,000 cells/cm^2 to 25 cm^2 of GelMA or collagen-coated polystyrene microcarriers in low attachment 6-well plates (Corning). After adjusting the volume of each well to a 5 mL with CCM, plates were agitated with a uniaxial rotor at 6 RPM (Mimetas™) for 22 hours in a cell culture incubator. The cells were harvested from the microcarriers by incubation with 0.25% trypsin/0.1% EDTA for 5 minutes at 37 ^{o}C, and the cells collected from the

collagen-coated polystyrene spheres were passed through a 40 μm cell strainer (PET mesh, PluriSelect). The cells were pelleted at 500 xg for 5 minutes and quantified using a hemocytometer.

2.2.8 Low-Attachment Well Plate Microcarrier Expansion

A total of 1,000 ihMSCs/cm^2 were seeded onto 25 cm^2 of GelMA microcarriers in low attachment 6-well plates according to the protocol in 2.2.7. Half of the media was exchanged every 2 days after collecting the microcarriers into 15 mL conical tubes and allowing them to settle. The cells were harvested on day 8 and counted according to the protocol listed in 2.2.7.

2.2.9 Vertical Wheel Bioreactor Expansion

A total of 1,000 ihMSCs/cm^2 were seeded onto 500 cm^2 of GelMA or collagen-coated polystyrene (Pall-Solohill) microcarriers in PBS-0.1MAG vertical wheel bioreactors (PBS Biotech) containing 100 mL CCM. ihMSCs were allowed to attach to microcarriers for 16 hours during on/off cycles of 12 RPM for 1 minute followed by 0 RPM for 20 minutes. After 16 hours, the bioreactor speed was increased to 17 RPM and changed to continuous operation. Bioreactor speeds for attachment and expansion were lower than those used in previous studies to minimize shear experienced during culture.[71,86] Every 2 days, half of the media in each bioreactor was replaced with fresh CCM after allowing the microcarriers to settle. On day 4, the speed of reactors containing collagen-coated polystyrene microcarriers was increased to 20 RPM to prevent microcarrier settling, while reactors containing GelMA microcarriers were

maintained at 17 RPM due to the lack of settling. These speeds were maintained until the end of the bioreactor expansion on day 8.

To assess expansion on the microcarrier surfaces, 10 mL aliquots of the GelMA or polystyrene microcarriers were removed every 2 days for ihMSC quantification. Microcarriers were washed with PBS and cells were removed via exposure to 0.25% trypsin/0.1% EDTA for 5 minutes at 37 ^{o}C with agitation. After deactivation of the trypsin with CCM, ihMSCs were separated from collagen-coated polystyrene microcarriers using a 40 µm cell strainer and pelleted at 500 xg for 5 minutes. Since GelMA microcarriers completely degraded during trypsin exposure, the cells did not require straining after trypsin deactivation and were directly pelleted. The number of ihMSCs was determined using a hemocytometer and divided by the microcarrier surface area to determine the degree of cell expansion.

After 8 days of expansion, microcarriers were removed from the reactor and allowed to settle in 50 mL conical tubes before aspiration of liquid culture media. Microcarriers were washed twice with 50 mL of PBS before the addition of 30 mL trypsin/EDTA and incubation for 5 minutes at 37 ^{o}C under 120 RPM agitation on an Advanced Digital Shaker (VWR). After the addition of culture media to deactivate trypsin, ihMSCs were separated from collagen-coated polystyrene microcarriers using a 40 µm cell strainer while ihMSCs isolated from GelMA microcarriers were not. Cells were collected after centrifugation at 500 xg for 5 minutes in CCM and concentration/viability was determined using trypan blue exclusion visualized on a hemocytometer.

2.2.10 Rotating Wall Vessel Bioreactor Expansion

A total of 1,000 ihMSCs/cm^2 were seeded onto 62 cm^2 of GelMA or collagen-coated polystyrene microcarriers in 10 mL RWVBs (Synthecon). ihMSC attachment occurred over 1 hour during on/off cycles of 24 RPM for 1 min followed by 0 RPM for 20 minutes. After this, the reactors were set for continuous operation at 24 RPM to ensure the microcarrier movement was minimized in the bulk fluid. Every 2 days, half of the media in each bioreactor was replaced with fresh CCM. Cells were expanded on microcarriers until day 6 or day 8, at which point they were washed twice with 10 mL PBS before exposure to 5 mL trypsin at 37 ^{o}C for 5 minutes with agitation. After trypsin deactivation with CCM, the cells were collected, strained according to the protocol in 2.2.9, and used for subsequent experiments.

2.2.11 Colony Forming Capabilities

Colony forming capabilities of recovered cells were determined as previously described.[87] Briefly, a total of 100 ihMSCs were seeded in 15 cm dishes with 20% (v/v) FBS-containing CCM and incubated for 21 days before staining with 3% (w/v) crystal violet in methanol. Colonies were counted by hand, and the number of colonies was divided by 100 to determine the percentage of cells in culture that were capable of self-replicating.[88]

2.2.12 Alizarin Red S Staining

Osteogenic differentiation was evaluated using previously described methods.[87,89] Briefly, cells were expanded in 12-well plates before exposure to osteogenic basal medium (OBM) consisting of 5 mM β-glycerophosphate (Sigma), 50

μg/mL ascorbic acid (Sigma), and CCM containing 20% FBS. Media was exchanged every 2-3 days to promote mineralization. After 21 days, monolayers were washed with PBS and fixed with 4% (w/v) paraformaldehyde (PFA) in PBS for 15 minutes. After fixation, monolayers were washed with PBS and deionized (DI) water before staining with 40 mM Alizarin Red S (ARS) in pH 4.0 water for 30 minutes. Residual ARS stain was washed with DI water and imaged using bright field microscopy. The amount of ARS in each well was quantified using absorbance at 405 nm after dye extraction using 10% (v/v) acetic acid in water.

2.2.13 Oil Red O Staining

Adipogenic differentiation was evaluated using previously described methods.[87] Briefly, cells expanded in 12-well plates were exposed to adipogenic differentiation medium (ADM) consisting of 500 nM dexamethasone (Sigma), 500 nM isobutylmethylxanthine (Sigma), 500 nM indomethacin (Sigma), and CCM containing 20% FBS. Media was exchanged every 3-4 days to promote lipid droplet formation. After 28 days of differentiation, monolayers were fixed with 4% (w/v) PFA in PBS and washed with PBS before staining with 0.6% Oil Red-O (ORO) in 60% isopropanol/40% PBS for 30 minutes. Monolayers were washed with PBS and imaged using bright field microscopy. Quantification of incorporated dye was performed using absorbance at 510 nm after extraction of dye with 100% isopropanol as previously described.[90]

2.2.14 Toluidine Blue Staining

Chondrogenic differentiation was evaluated using previously described methods.[87] Briefly, 200,000 ihMSCs were pelleted in 15 mL conical tubes in either

CCM with 20% FBS or in chondrogenic differentiation medium (CDM) consisting of High-glucose DMEM (Invitrogen), 100 nM dexamethasone, 50 µg/mL ascorbate 2-phosphate (Sigma), 40 µg/mL proline (Sigma), 100 µg/mL pyruvate (Sigma), 500 ng/mL Bone Morphogenetic Protein-2 (BMP-2), 10 ng/mL Transforming Growth Factor-β3 (TGF-β3), and insulin, transferrin, selenium (ITS)+ Premix (Corning). Media was exchanged every 3 days for 21 days, at which point the pellets were washed with PBS and fixed with 4% PFA. After measuring the diameter, pellets were embedded in parrafin, cut in 10 µm sections, placed on microscope slides, and stained with Toluidine-Borate. Images of the sections were acquired using bright field microscopy.

2.2.15 EV Purification

After 8 days of expansion in RWVBs or vertical wheel bioreactors, ihMSC-laden microcarriers were washed twice with PBS and incubated in 10 mL or 60 mL of a previously-described chemically defined (CDPF) medium for 24 hours to promote EV generation.[25,91] After passing the media supernatants through a 0.2 µm PES filter and concentration using Vivaspin™ tubes (10 kDa MWCO, GE Healthcare, Chicago, IL), EVs were collected via ultracentrifugation at 100,000 ×g for 16 hours at 4 ^{o}C using a Sorvall WX Floor Ultracentrifuge with an AH-629 36-mL swinging bucket rotor (Thermo Scientific). EV pellets were resuspended in PBS, and particle size and concentration were determined using a NanoSight LM-10 nanoparticle tracking system (Malvern). The remaining suspended EVs were stored at -80 ^{o}C until further use.

2.2.16 Immunomodulatory Potential

The immunomodulatory potential of isolated ihMSCs and secreted EVs were evaluated using *in vitro* LPS stimulation of murine splenocytes as previously described.[25,91,92] Splenocytes (5×10^5 cells/well) isolated from 6-week old BALB/c or C57BL/6J mice (Jackson Laboratory, Bar Harbor, ME) mice were stimulated with 50 ng/mL LPS in RPMI containing 5% heat-inactivated FBS with 100 U/mL penicillin/100 mg/mL streptomycin. The splenocytes were mixed with ihMSCs (2.5×10^3, 5×10^3 and 10×10^3 cells/well) plated the day before or with the indicated number of EVs. After 24 hours, the concentration of IFN-γ, IL-6, TNF-α in cell-free supernatant was determined using ELISA in triplicate according to the manufacturer's protocol. Three wells of splenocyte culture were used as technical replicates.

2.2.17 Cost Analysis

An analysis was performed to determine the cost of disposable reagents for the production of GelMA microcarriers using the two different microfluidic devices available in this study. Costs were determined using the required reagents for the production of 20 mL of GelMA microcarriers. The production costs were normalized to microcarrier surface area and compared to the costs of commercial microcarriers.

2.2.18 Statistics

Statistical differences between groups were evaluated and deemed significant at p-values less than 0.05. Differences in attachment densities was measured using two-way ANOVA with Tukey's multiple comparisons test. Differences in cell densities in low-attachment plates and PBS bioreactors were determined using two-tailed t-tests.

Differences in expansion between the two microcarrier cultures was evaluated using a repeated measures ANOVA, and differences between cell densities on each day were determined using Sidak's multiple comparison test. Difference in cell viability after harvest from the PBS bioreactor was determined using two-tailed t-tests. Differences in ARS and ORO intensity were measured using a one- or two-way ANOVA with Tukey's multiple comparisons test. Differences in cytokine secretion in the murine splenocyte assay were determined using a one-way ANOVA with Dunnett's or Tukey's multiple comparisons test.

2.3 Results

2.3.1 GelMA Microcarrier Production Using Step Emulsification

Microcarriers were initially produced using a coaxial flow focusing device that has been used previously in the lab for the production of GelMA microcarriers.[85] The microcarriers had an average diameter of 73 ± 23 μm and were able to be isolated effectively from mineral oil with an overall recovery of only ~20%. A 100-channel step emulsification microfluidic device was evaluated for further experiments due to previous studies demonstrating higher production rates of more uniform microcarriers with lower flowrates for the oil phase (Figure 2-3 A-B).[93]

The maximum flowrate for production of monodisperse droplets in a step emulsification depends on the viscosity of the aqueous solution[21]. Using isothermal rheology, the viscosities of 4% and 7.5% GelMA prepolymer at 40 ^{o}C and a shear strain of 1/sec were 2.65 and 6.07 mPa*s, respectively. These readings may not be representative throughout the microfluidic device, as GelMA solutions are shear thinning

and thus susceptible to shear stress and strain.[94] These viscosities are predicted to result in jetting for flowrates above 6 and 3 mL/hr for 4% and 7.5% GelMA, respectively.[93] To ensure the microfluidic device was not operating in the jetting regime, the GelMA flowrate was set to 2 mL/hr.

Microcarriers produced from both 4% and 7.5% GelMA had uniform diameters of approximately 120 μm that followed normal distributions with coefficients of variation less than 5% (Figure 2-3 C-D). In addition, though the diameter of the 4% and 7.5% GelMA microcarriers appeared to increase during 2 hours of continuous production, the average diameters were always within one standard deviation of one another (Figure 2-3 E). Based on these results, GelMA microcarriers were prepared using step emulsification microfluidics for subsequent experiments.

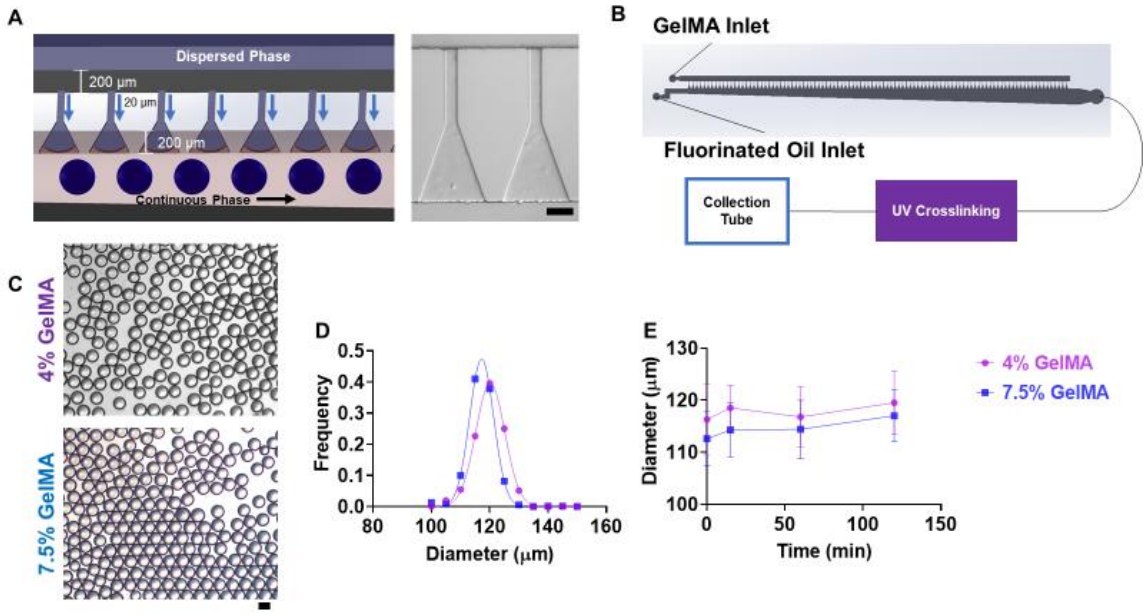

Figure 2-3: Uniform GelMA Droplets are Generated Using Step Emulsification Microfluidics
(A) A schematic of the microfluidic device demonstrates the dimensions and the flow pattern of the GelMA (Dispersed) phase and the fluorinated oil (Continuous) phase. (B) A diagram of the microcarrier production process indicates the location of UV crosslinking between droplet generation and collection. Not shown in this diagram is that the GelMA, fluorinated oil, and microfluidic device were maintained in a 40 ^{o}C heated environment. (C) Bright field images of 4% and 7.5% GelMA microcarriers demonstrate uniform diameter distributions after crosslinking and collection. (D) Microcarriers prepared from 4% and 7.5% GelMA adopt normal diameter distributions around 120 µm. Additionally, there was an appreciable degree of overlap between the two microcarrier preparations. (E) Average and variance of microcarrier diameters did not appreciably changeover 2 hours of production. Data presented in this figure is representative of three independent microcarrier productions. Scale bars represent 100 µm. Reprinted from [95].

We also determined that the compressive modulus of bulk hydrogels made from 4% and 7.5% GelMA were 0.98 ± 0.36 kPa and 8.15± 0.65 kPa, respectively. To relate the bulk modulus measurements to that of an individual microcarrier, we measured the force-displacement relationship of a 4% GelMA microcarrier. A Hertz model fit (red) to the indentation curve (blue) indicated an elastic modulus of 2.5 kPa (Figure 2-4 A).

Applying a constant compressive strain to the microcarrier resulted in minimal stress relaxation, indicating the microcarrier largely behaved like an elastic solid (Figure 2-4 B). Nanoindentation was not performed on 7.5% GelMA microcarriers due to sample loss prior to the measurement at an off-site facility.

Incubation of the collected microcarriers with commercially available proteases demonstrated complete degradation of microcarriers by trypsin and TrypZEAN™ after 5 minutes, while Accutase™ did not degrade the microcarriers even after 15 minutes (Figure 2-4 C).

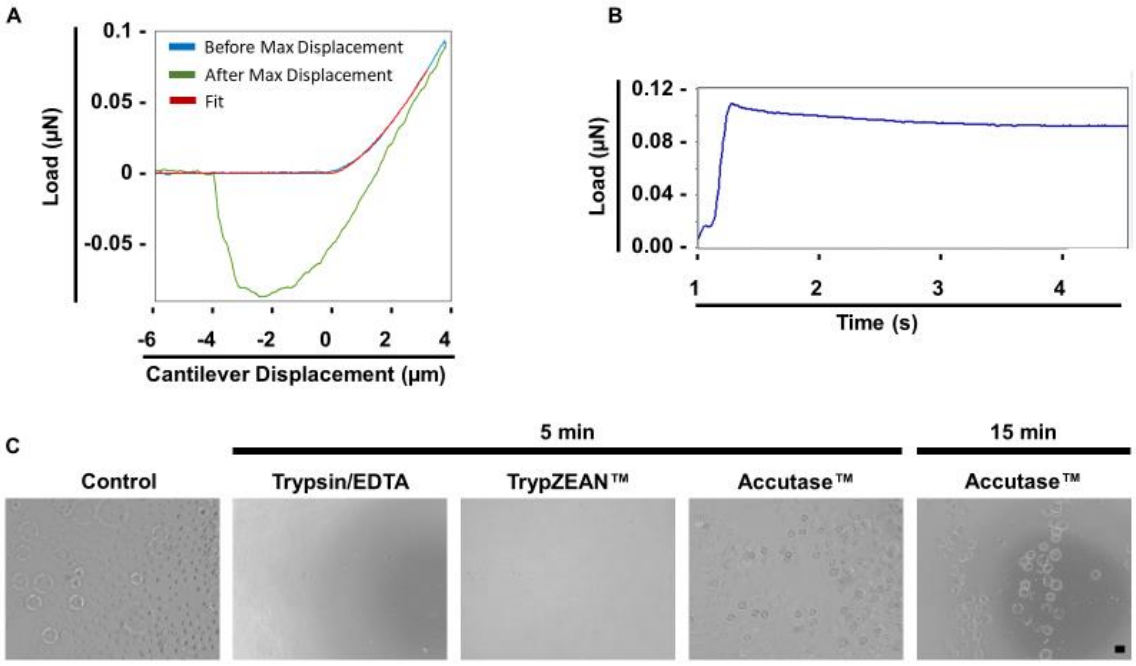

Figure 2-4: GelMA Microcarriers are Elastic And Proteolytically Degradable
(A) Nanoindentation analysis of 4% GelMA microcarriers demonstrates an elastic modulus of 2.5 kPa. (B) Stress-relaxation curve of 4% GelMA microcarriers demonstrates low relaxation of compressive load with constant strain. (C) Representative images of 4% GelMA microcarriers after incubation with the indicated protease at 37 ^{o}C demonstrate complete degradation of microcarriers by 5 minutes when incubated with 0.25% trypsin/0.1% EDTA or 0.05% TrypZEAN™. Meanwhile, microcarriers incubated with Accutase™ were not degraded even after 15 minutes of incubation, though the

number of microcarriers appears to decrease as a function of time. Scale bar represents 100 μm.

2.3.2 ihMSC Expansion on GelMA Microcarriers

Optimal seeding densities of ihMSCs on 4% and 7.5% GelMA microcarriers compared to collagen-coated polystyrene microcarriers were determined using pilot experiments performed in low-attachment well plates. After 22 hours, the cells seeded at 1,000 and 5,000 cells/cm^2 had 100% recovery. The recovery of ihMSCs after initially seeding at 10,000 cells/cm^2 was approximately 80% in all tested microcarrier conditions. The density of recovered cells from collagen-coated polystyrene microcarriers trended lower than the GelMA microcarriers in all three conditions (Figure 2-5 A).

The comparison of ihMSC expansion potential on 4% and 7.5% GelMA microcarriers in low-attachment plates over 8 days resulted in a maximal cell density of approximately 15,000 cells/cm^2. The final density was identical regardless of whether cells were seeded at 6,600 cells/cm^2, a seeding density similar to those used in other studies, or 1,000 cells/cm^2 (Figure 2-5 B).[71]

To determine whether the same degree of expansion was possible in a vertical wheel bioreactor, 8-day expansions were performed with 4% and 7.5% GelMA microcarriers seeded with 1,000 ihMSCs/cm^2. Three-fold fewer ihMSCs were recovered from 4% GelMA microcarriers than 7.5% GelMA microcarriers (Figure 2-5 C). As a result, only 7.5% GelMA microcarriers were used for subsequent vertical wheel bioreactor experiments. The experiment was repeated to compare the degree of expansion between 7.5% GelMA microcarriers and collagen-coated polystyrene microcarriers. Expansion of ihMSCs was similar on both microcarriers, and viability was not different in the cells

recovered in either condition (Figure 2-5 D-E). Millimeter-sized microcarrier aggregates were observed on days 6 and 8 of expansion on 7.5% GelMA microcarriers. Live/dead staining demonstrated no apoptotic cells in the center of the aggregates (Figure 2-5 F).

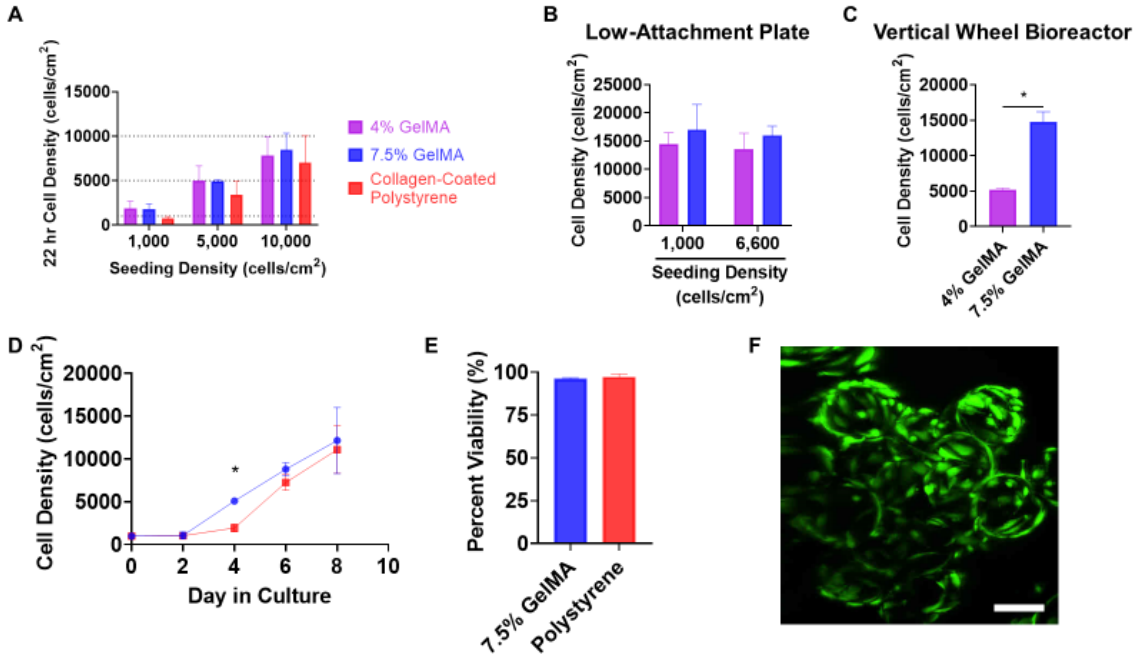

Figure 2-5: GelMA Microcarriers Are a Suitable Scaffold for ihMSC Expansion in Vertical Wheel Bioreactors

(A) The number of ihMSCs recovered after 22 hours of microcarrier culture in low attachment plates yielded similar quantities to the initial number added. Dashed lines were added indicating the original seeding densities to ease comparison between the two time points. (B) Expansion of ihMSCs over 8 days on 4% and 7.5% GelMA microcarriers in low attachment plates resulted in final cell densities around 15,000 cells/cm^2 regardless of the original seeding density. (C) The expansion of ihMSCs on 4% GelMA microcarriers in PBS bioreactors was significantly lower than the expansion on 7.5% GelMA microcarriers. (D) Expansion curves between 7.5% GelMA and collagen-coated polystyrene microcarriers demonstrated over 10-fold expansion over 8 days in PBS bioreactors. There was a significantly increased number of cells recovered from 7.5% GelMA on Day 4, but the two expansion curves were not statistically different. (E) The viability of cells recovered from GelMA and collagen-coated polystyrene microcarriers was higher than 95%. A representative image of Live/Dead stained ihMSCs on GelMA microcarriers after 8 days of expansion is shown in (F). Data presented in this figure are generated from at least three independent cultures. Differences between final cell densities of each microcarrier group at specific seeding densities in (A) was evaluated using one-way ANOVA. Differences between cell

densities in (B) were evaluated using two-way ANOVA. The differences between cell numbers and viability in (C) and (E) were evaluated using two-tailed t-tests. Differences between expansion curves in (D) were evaluated using a repeated-measures ANOVA, with the means on each day being compared via Sidak's multiple comparisons test. * indicates statistically different values at $p<0.05$. Reprinted from [95].

2.3.3 Validation of Stem Cell Identity

After isolation from the microcarriers, the identity of ihMSCs was verified according to clonogenicity and differentiation potential, components of the ISCT hMSC criterion.[20] Following bioreactor expansion, the colony forming potential of ihMSCs expanded on 7.5% GelMA or collagen-coated polystyrene microcarriers was not significantly different than monolayer-expanded ihMSCs (Figure 2-6 A-B). Furthermore, ihMSCs adopted a spindle-shaped morphology with a majority having a central halo on phase contrast microscopy, features typical of hMSCs. These features were present regardless of whether cells were cultured on either microcarrier (Figure 2-6 C). Clonogenic potential was similar during pilot experiments of ihMSCs expanded on 4% GelMA and 7.5% GelMA microcarriers in Rotating Wall Vessel Bioreactors (RWVBs), where 7.5% GelMA microcarrier and monolayer cultures had similar colony forming potentials, while 4% GelMA microcarrier cultures were significantly lower than the other two groups (Figure 2-6 D-E).

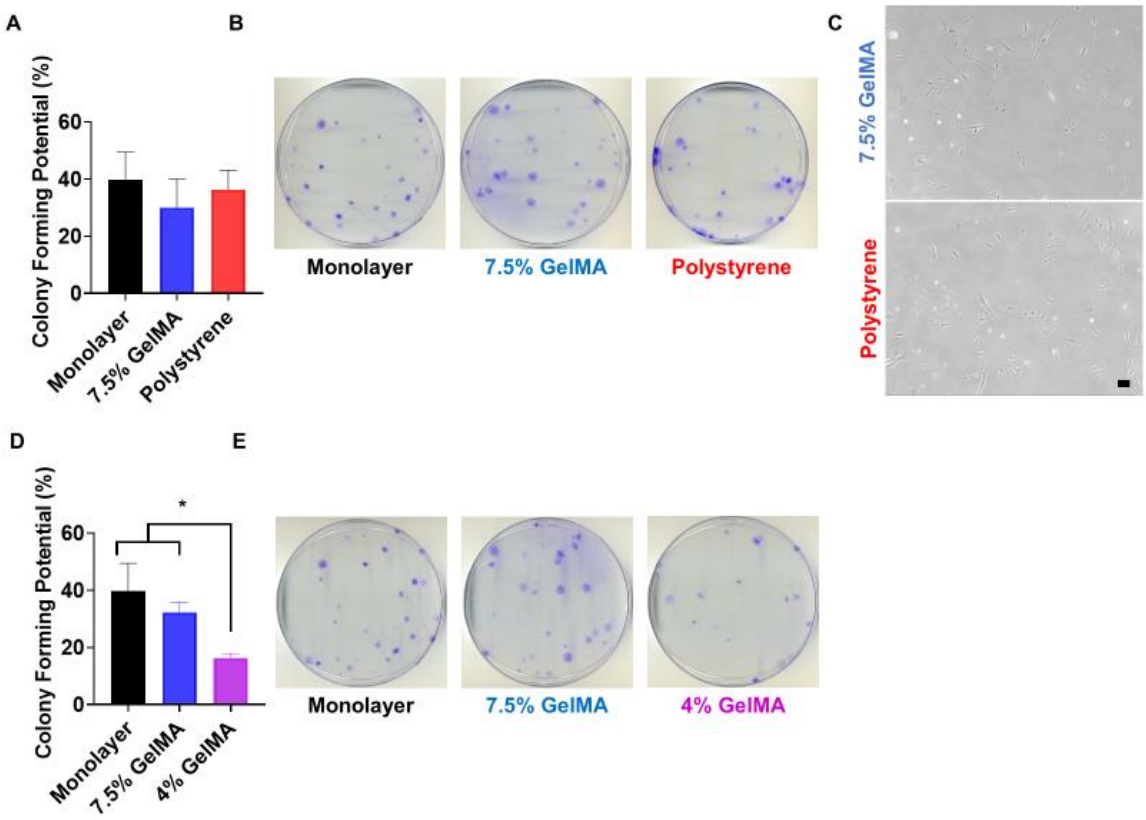

Figure 2-6: The Clonogenicity of ihMSCs is Maintained on all Microcarrier Surfaces but 4% GelMA After Expansion
(A) Colony forming capabilities of ihMSCs are not significantly different between monolayer and microcarrier expansion. Representative images of plates from the colony forming assay are shown in (B). (C) Images of ihMSC monolayer culture 4 days after bioreactor isolation demonstrate that the recovered cells do not significantly alter their morphology compared to monolayer culture. (D) Quantification of colony forming potential demonstrates that ihMSCs expanded on 4% GelMA microcarriers form fewer colonies than those expanded on 7.5% GelMA microcarriers or monolayer. (E) Representative images of colony forming plates in (D). A total of three plates per condition were used for generating the data in (A) and (D). Scale bar represents 100 µm. * indicates statistical significance at $p<0.05$. Reprinted from [95].

The osteogenic differentiation potential of ihMSCs was maintained after microcarrier expansion in vertical wheel bioreactors, with dense ARS staining of mineralized monolayers (Figure 2-7 A-B). The amount of ORO staining in ADM-treated ihMSCs appeared slightly increased visually compared to CCM-treated cells, though

absorbance readings of extracted dye were not significantly different between either culture condition (Figure 2-7 C-D). Finally, increased toluidine blue staining and the formation of lacunae was observed after culture in chondrocyte differentiation medium in monolayer and polystyrene cultures. Clusters of cells separated by vacant space were observed after CDM culture of 7.5% GelMA microcarriers (Figure 2-7 E).

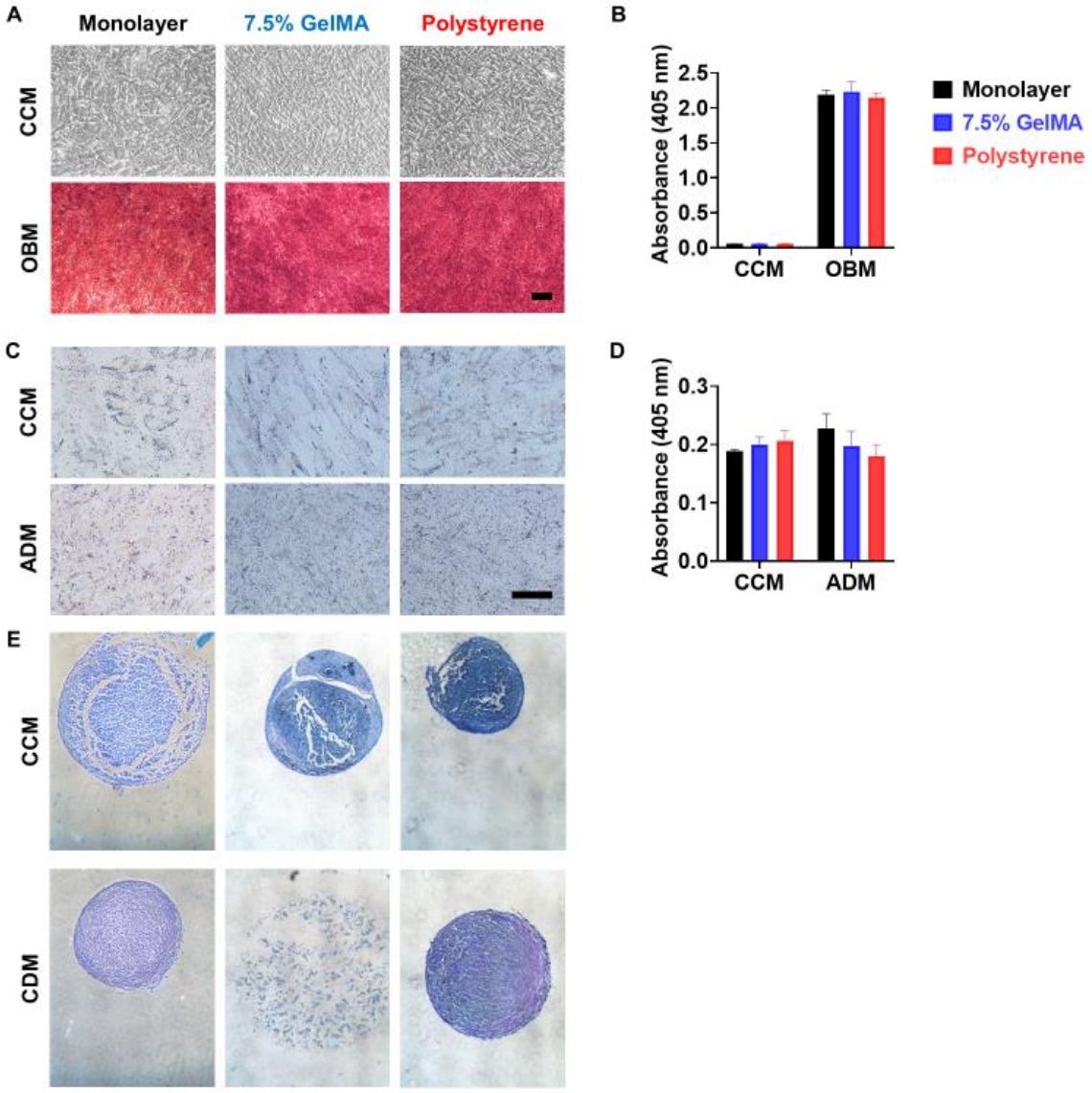

Figure 2-7: Trilineage Differentiation Potential of ihMSCs is Maintained After Microcarrier Expansion

(A) Representative images of ARS-stained monolayers after 21 days of culture demonstrate robust mineralization in ihMSCs expanded on 7.5% GelMA and collagen-coated polystyrene microcarriers, with the observed staining intensity similar to monolayer-expanded ihMSCs. (B) There was no difference between the absorbance of ARS extracts prepared from mineralized monolayers. (C) Representative images after 28 days of culture in ADM appears to increase the number of ORO droplets compared to ihMSCs maintained in CCM. (D) There was no statistically significant difference in absorbance of extracted ORO dye between culture supplement or microcarrier surface. ARS and ORO dye were extracted from three different wells for quantification. Statistical differences in ARS absorbance intensity were determined using one-way

ANOVA with Tukey's multiple comparison test, while differences in ORO were determined using two-way ANOVA with Tukey's multiple comparison test. Statistical relevance was evaluated at $p<0.05$. Reprinted from [95]

The osteogenic and adipogenic differentiation observed in the vertical bioreactors was similar to differentiation observed after RWVB expansion on 4% and 7.5% GelMA microcarriers and cells grown in monolayer (Figure 2-8 A-B). Robust mineralization and ARS staining were observed after osteogenic differentiation in ihMSCs recovered from both microcarriers, while there appeared to be a small increase noted visually in ORO staining after adipogenic differentiation that was insignificant upon quantification (Figure 2-8 C-D).

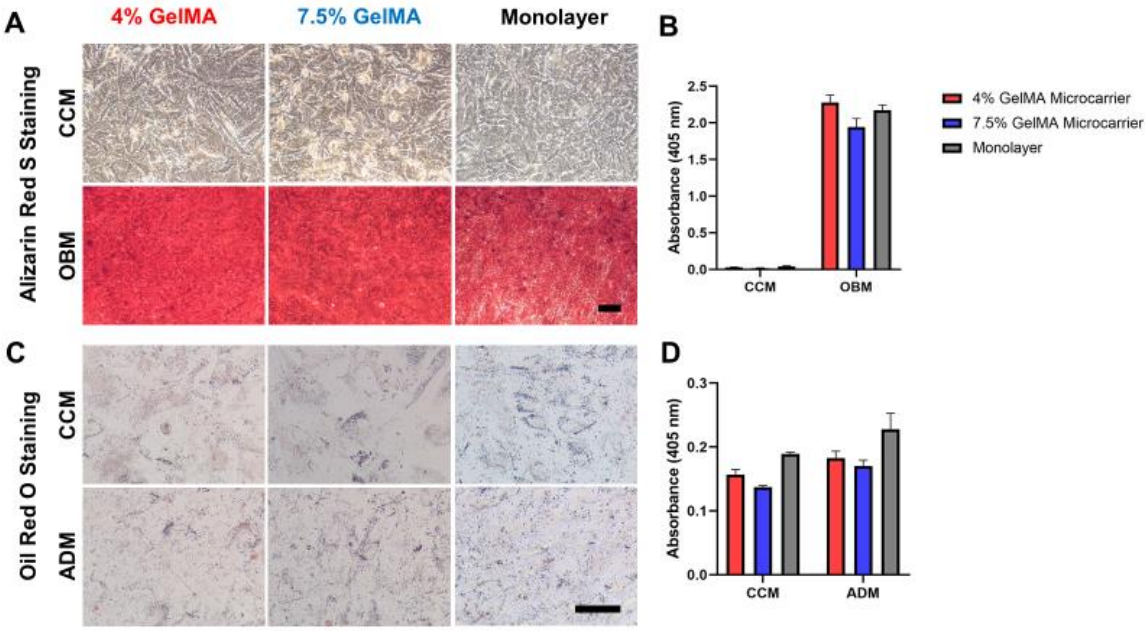

Figure 2-8: Osteogenic and Adipogenic Differentiation Potential Are Preserved After RWVB Expansion on GelMA Microcarriers
(A) Representative images of ARS stained monolayers after 21 days of culture demonstrate robust mineralization in ihMSCs expanded on 4% and 7.5% GelMA microcarriers in RWVBs, with the observed staining intensity similar to monolayer-

expanded ihMSCs. (B) There was no difference between the absorbance of ARS extracts prepared from mineralized monolayers. (C) Representative images after 28 days of culture in ADM appears to increase the number of ORO droplets compared to ihMSCs maintained in CCM. (D) No significant difference was observed between extracts of the ORO from the wells in (C). Dye was extracted from three wells for quantification. Statistical differences in Alizarin Red S absorbance intensity were determined using one-way ANOVA with Tukey's multiple comparison test, while differences in Oil Red O were determined using two-way ANOVA with Tukey's multiple comparison test. Statistical relevance was evaluated at $p<0.05$. Reprinted from [95]

2.3.4 EV Production and Immunomodulatory Characteristics

A series of pilot experiments were performed after RWVB culture to determine whether microcarrier expansion altered the capability of ihMSCs or ihMSC-EVs at inhibiting cytokine secretion from murine splenocytes after LPS stimulation. Cells and EVs isolated from 7.5% GelMA microcarriers after RWVB cultures were able to dose-dependently reduce splenocyte secretion of IFN-γ and IL-6 (Figure 2-9 A-D). Additionally, at several ihMSC:splenocyte ratios, cells isolated from 7.5% GelMA microcarriers suppressed IFN-γ secretion to a higher degree than cells recovered from monolayer or collagen coated polystyrene microcarriers (Figure 2-9 A). Additionally, cells isolated from 7.5% GelMA and collagen-coated polystyrene were more potent at suppressing IL-6 expression at the lowest ihMSC:splenocyte ratio (Figure 2-9 C).

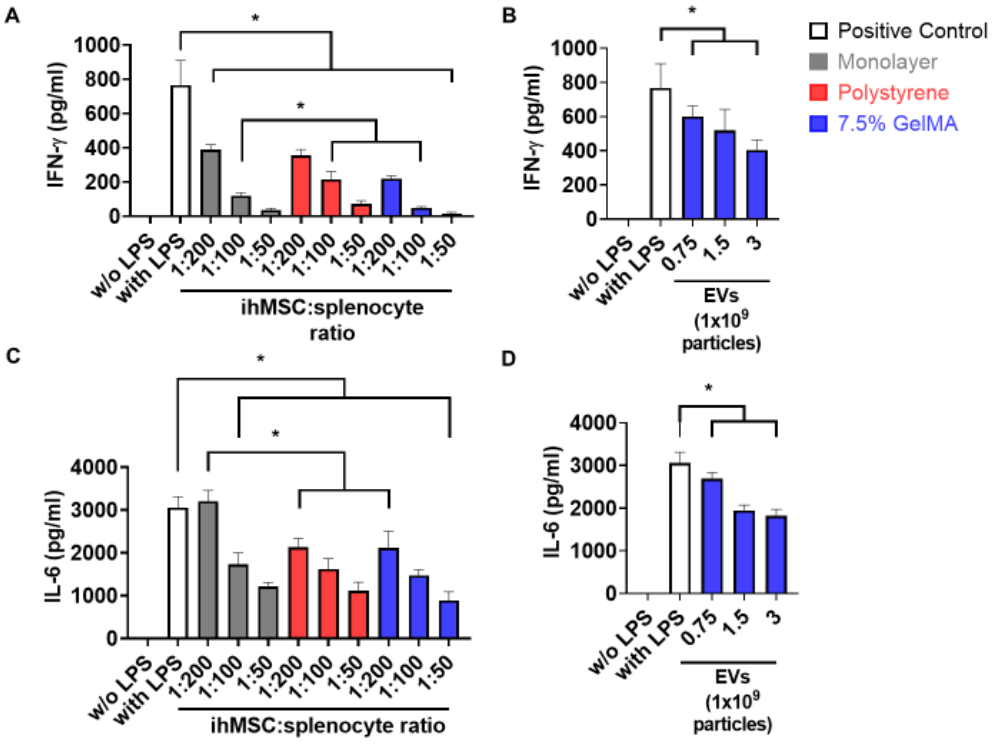

Figure 2-9: GelMA Microcarrier Expansion in RWVBs Enhances or Preserves Immunomodulatory Capabilities of ihMSCs and EVs
(A) Quantification of 24 hour IFN-γ release demonstrates that ihMSCs expanded on 7.5% GelMA microcarriers are more potent immunomodulators than ihMSCs expanded on collagen-coated polystyrene microcarriers or monolayer culture. (B) EVs isolated from 7.5% GelMA microcarriers are able to reduce IFN-γ release independently. (C) Quantification of 24-hour IL-6 release demonstrates that ihMSCs grown on 7.5% GelMA or collagen-coated polystyrene microcarriers are more potent than monolayer-cultured ihMSCs. (D) EVs isolated from 7.5% GelMA microcarriers are able to independently reduce the release of IL-6. * indicates statistical difference at $p<0.05$. Reprinted from [95]

After the findings of our pilot experiments, EVs and cells were harvested after expansion using PBS bioreactors. The recovered ihMSCs were able to suppress the expression of IFN-γ, IL-6, and TNF-α, though the cells from microcarriers were not as potent as monolayer cultured cells when hMSCs and splenocytes were added in 1:100 dilutions (Figure 2-10 A-C).

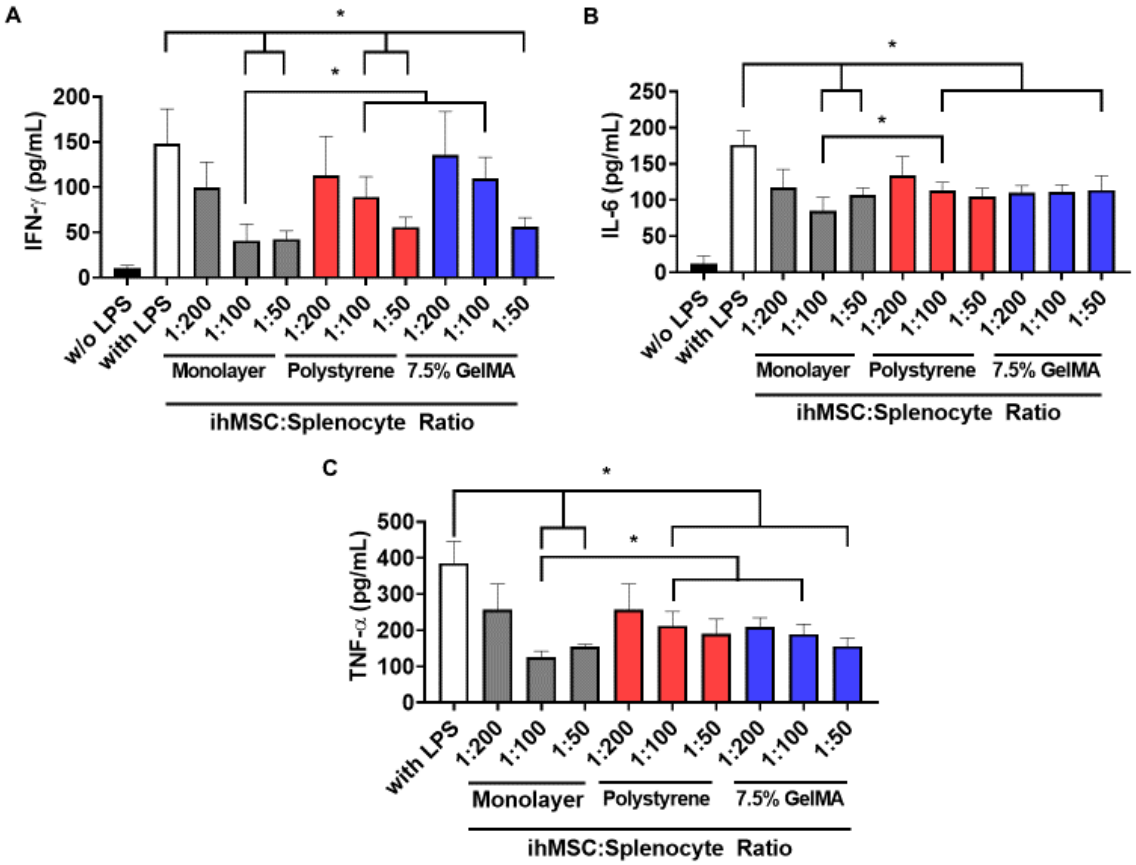

Figure 2-10: Vertical Wheel Bioreactor Expansion Produces Immunomodulatory ihMSCs
(A) IFN-γ ELISA demonstrates ihMSCs from monolayer and collagen-coated polystyrene microcarrier culture are more potent at suppressing IFN-γ excretion than ihMSCs from GelMA microcarriers. (B) IL-6 ELISA demonstrates suppression of IL-6 in all three ihMSC groups. (C) TNF-α ELISA demonstrates all three cell conditions are capable of suppressing TNF-α secretion. Differences from the positive control in (A)-(C) were measured using a one-way ANOVA with Dunnett's post-hoc analysis. Differences between groups at corresponding dilutions were measured using a one-way ANOVA with Tukey's post-hoc analysis. * indicates statistical significance at $p<0.05$. Reprinted from [95].

The number of recovered EVs was two-fold higher from GelMA microcarriers than collagen-coated microcarriers in vertical wheel bioreactors. (Figure 2-11 A). The average mean diameters between EVs were similar to one another, with monodisperse diameters present in each preparation (Figure 2-11 B-C). However, EV purifications

from either monolayer or either microcarrier expansion were unable to consistently reduce the secretion of either IFN-γ or IL-6 (Figure 2-11 D-E).

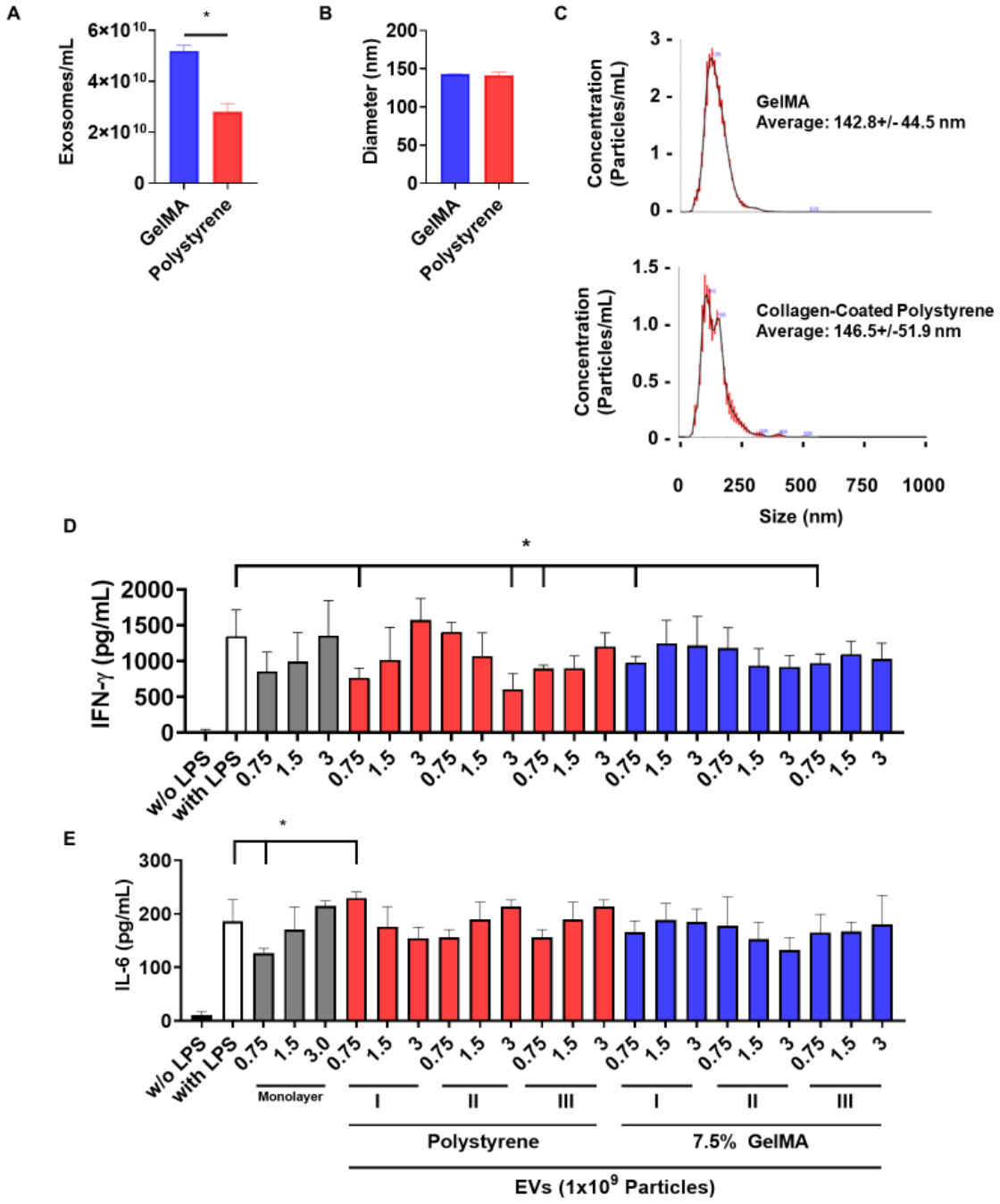

Figure 2-11: Vertical Wheel Bioreactor Expansion on GelMA Microcarriers Increases Production but Inhibits Immunomodulatory Potential of EVs
(A) Twice the number of EVs are isolated from GelMA microcarrier cultures than polystyrene cultures in vertical wheel cultures. (B) The diameter of recovered EVs are the same from both bioreactors. (C) Representative histograms of recovered EVs demonstrate appropriate size distributions. (D) No significant pattern is found in

suppression of IFN-γ with EV treatment from either monolayer or microcarrier conditions. (E) EVs isolated from either monolayer or microcarrier were not consistently able to inhibit IL-6 secretion. Differences between exosome concentrations in (A) were measured using two-tailed t-tests. Differences from the positive control in (D) and (E) were measured using a one-way ANOVA with Dunnett's post-hoc analysis and between each ihMSC:splenocyte ratio in using a one-way ANOVA with Tukey's post-hoc analysis. * indicates statistical significance at $p<0.05$. Reprinted from [95].

2.3.3 Cost Analysis of Microcarrier Production

A cost analysis comparing the two microfluidic device techniques is shown in Table 1. The cost to produce 20 mL of microcarriers was $312.81 for the flow focusing device and $103.14 for the step emulsification device. The reason in the reduction of cost was the recycling of fluorinated oil in step emulsification. When normalized to surface area, the cost to generate both sets of microcarriers cm^2 of culture area was lower than the value for purchasing the commercially available microcarriers used in this manuscript, which were 28.2 cents per cm^2.

Table 1: Cost Analysis of Production for 20 mL of 7.5% GelMA Microcarriers Between Flow-Focusing and Step Emulsification Devices

	Microfluidic Device Platform Assume Production of 20 mL 7.5% GelMA Microcarriers	
	SLA Flow-Focusing Device	100-Channel Step Emulsification
Oil	Mineral Oil	Novec7500
Surfactant	Span-80	PicoSurf-1
Surfactant Concentration Percent (v/v)	1	1
Total Cost ($/mL)	**0.075**	**8.698**
GelMA Cost ($/g)	4.107	4.107
LAP Concentration (mg/mL)	10	2.94
LAP Cost ($/mL GelMA)	1.19	0.349
Oil Flowrate (mL/min)	0.25	0.067
GelMA Flowrate (mL/min)	0.01	0.033
Recovery	20%	70%
Time (min)	10000	857.1
Oil Used (mL)	2500	57.14
GelMA Used (mL)	100	28.57
Oil Lost (mL)	2500	14.29
Total Cost for 20 mL GelMA ($)	**312.8**	**140.4**
Average Diameter (um)	73	120
StDev Diameter (um)	23	6
SA (cm^2)	1.674E-04	4.524E-04
Volume (mL)	2.036E-07	9.047E-07
Spheres in 10 mL	9.819E+07	2.210E+07
Total SA (cm^2)	**16438**	**10000**
Cost per cm2 ($/$cm^2$)	**0.019**	**0.010**

2.4 Discussion

In this study, we demonstrated that GelMA microcarriers support the expansion of ihMSCs in RWVBs and vertical wheel bioreactors without losing clonogenic or differentiation potential. Isolation of ihMSCs after bioreactor expansion on GelMA microcarriers could also be accomplished through direct dissolution of the microcarriers, thus avoiding use of cell strainers. ihMSCs and EVs recovered from RWVBs after

GelMA microcarrier culture showed at least comparable, if not greater, immunomodulatory potential than monolayer-cultured cells.

The use of step emulsification microfluidic devices for the generation of microcarrier batches is appealing due to their ability to maintain low variations in droplet diameter despite variations in flowrate.[93,96] The 100-channel device used in this study was able to produce uniform 120 µm microcarriers over two hours of continuous production, similar to observations in previous publications.[96] We also demonstrated that the cost to generate GelMA microcarriers with step emulsification microfluidics was lower than that of purchasing commercial microcarriers, even at the scale needed to operate a 2 L bioreactor. The maximum operating flowrates in step emulsification microfluidics are directly proportional to the number of channels, so 500 channels permit the production of 10,000 cm^2 microcarrier surface area after 2 hours of operation - enough to operate a 2 L bioreactor.[93] Future experiments should focus on optimizing the purification of GelMA microcarriers, including the use of microfluidic devices or filters to further collect oil for recycling.[40]

Vertical wheel bioreactors and RWVBs were used since they minimize shear forces experienced during expansion since shear forces have been shown to be detrimental to hMSC expansion.[97-101] RWVBs minimize shear forces by causing the cell culture media and microcarriers to rotate as a fluid mass though rotational acceleration of the entire reactor.[102] Oxygen and carbon dioxide (CO_2) transport occurs via diffusion through a semi-permeable silicon membrane, thereby preventing hypoxia in the culture environment. The impeller design in the vertical wheel bioreactor homogenizes fluid and

hydrodynamic forces by mixing in both axial and radial directions simultaneously.[99] In addition, vertical wheel bioreactors can ensure adequate mixing with lower power inputs, avoiding turbulent mixing seen in stirred tank and rocking bag reactors.[99]

Though we demonstrated ihMSCs expanded to similar densities on 4% and 7.5% GelMA microcarriers when cultured in low attachment plates, there was a three-fold decrease in expansion on 4% GelMA microcarriers compared to 7.5% GelMA and collagen-coated polystyrene when cultured in vertical wheel bioreactors. We originally pursued the use of 4% GelMA microcarriers for cell expansion as previous studies have demonstrated cell expansion in well plates after cell encapsulation in 4-5% GelMA hydrogels.[37,103,104] However, the translation of 4% GelMA from low-attachment plates to vertical wheel bioreactors led to a three-fold decrease in the number of recovered cells after normalization to culture area.

The clonogenicity and trilineage differentiation validation assays in this study have been used in previous studies after bioreactor hMSC expansion.[71,73,105-108] The lack of chondrogenic staining in the cell pellet formed after GelMA microcarrier expansion could be attributed to the detachment of the section during staining. To address this issue, adhesive microscope slides could be used to ensure the section remains attached to the slide, or mRNA extracts can be prepared for qRT-PCR analysis of genes expressed during chondrogenesis, including the transcription factor Sox9 and extracellular proteins Collagen II, Aggrecan, and Collagen Oligomeric Matrix Protein.[109] Other validation techniques such as metabolite analysis during expansion can assist in evaluating culture health and media exchanges in future experiments.[71,73,107]

In conclusion, we have demonstrated that GelMA microcarriers can serve as a degradable scaffold for hMSC expansion in scalable reactors while preserving stem cell identity and immunomodulatory potential. Additionally, EV production was greater during GelMA microcarrier culture than on monolayer or collagen-coated polystyrene culture. Though the EVs prepared after vertical wheel bioreactor expansion were not effective at suppressing LPS-induced splenocyte activation, they may be effective in other models of immune activation such as *in vitro* mixed lymphocyte reactivity assays.[110] GelMA microcarriers can be produced using step emulsification microfluidic devices for lower prices than the purchase of commercial microcarriers. Future studies include immunophenotyping of produced cells and analyzing the chondrogenesis of ihMSCs GelMA microcarrier expansion, optimizing conditions for larger-scale bioreactor operations, particularly GelMA microcarrier production using step emulsification microfluidics and ihMSC culture conditions, and validation of the *in vitro* findings in this manuscript with *in vivo* models of inflammatory disorders.

CHAPTER 3

EVALUATION OF HUMAN PLATELET LYSATE AS A XENO-FREE SUPPLEMENT FOR IMMUNOMODULATORY APPLICATION OF INDUCED PLURIPOTENT STEM CELL-DERIVED MESENCHYMAL STEM CELLS

3.1 Introduction

hMSCs and hMSC-derived EVs are emerging as therapeutic options for various disorders, including diseases of innate and adaptive immune regulation.[6,111] However, FDA recommendations have prompted cell therapeutic culture to adopt xeno-free culture conditions.[52,112] Therefore, using animal/xeno-free media is becoming an expectation for manufacturing therapeutic hMSC products, including ihMSCs.

hPL is an animal-free supplement effective for ihMSC expansion.[55,113] Supplementation with hPL instead of FBS also reduces therapeutic production costs by increasing hMSC expansion relative to that obtained using FBS.[17,114] However, there have been conflicting reports about maintenance of hMSC immunomodulatory potential after hPL supplemented expansion.[53] A direct comparison between the immunomodulatory potential of ihMSCs grown in hPL- or FBS-supplemented media has not been reported.[18,51,115-118]

Another improvement to the current state of cell therapy for immunologic diseases is the proposed use of cell-free products.[23,68] Though ihMSCs have shown promise as a treatment option for immune-related diseases, the use of ihMSC-derived EVs avoids the risk of engraftment and alloimmunization.[119] Media supplemented with hPL has been used for the expansion and purification of EVs from BM-hMSCs, though

the immunomodulatory potential was not evaluated.[120] EVs isolated from ihMSCs expanded in FBS have immunosuppressive effects in several *in vitro* and *in vivo* inflammatory models.[25,92] The immunosuppressive potential of EVs harvested from ihMSCs expanded in hPL has not been characterized.

We hypothesized that culture of ihMSCs in hPL will improve or maintain expansion capabilities and immunomodulatory potential of cells and EVs compared to culture in FBS. Protocols for hPL preparation were compared to identify the technique with the highest recovery of purified hPL with potential for cGMP production. Initial experiments with hPL-supplemented media were performed in BM-hMSCs to assess expansion and differentiation capabilities. Subsequent experiments used hPL-supplemented media in ihMSC culture to assess expansion, colony forming potential, and trilineage differentiation. Immunomodulation experiments were performed with ihMSCs and both production and immunomodulation experiments were performed in ihMSC-derived EVs after expansion in either FBS- or hPL-supplemented media.

3.2 Methods

3.2.1 Platelet Lysate Production

hPL units were prepared using either expired whole-blood-derived platelet units (American Red Cross) for BM-hMSC culture or apheresis units (Children's Healthcare of Atlanta) for ihMSC culture. Upon arrival, the platelet units were frozen at -20 ^{o}C until processing. The platelet units were lysed using two freeze-thaw cycles between -20 ^{o}C and 37 ^{o}C before they were pooled according to their donation type (whole-blood-derived versus apheresis) and stored in 50 mL conical tubes at -20 ^{o}C until use. When

they were ready for use, platelet lysates were centrifuged at 3,000 xg for 20 minutes to pellet insoluble particulate material, and the supernatant was prepared for preparing cell culture media using different protocols.[49,63,121] Briefly, the protocols to prepare platelet lysate supplement were performed as follows:

A) Sterile calcium chloride (1 M in deionized water) was added to the platelet lysate supernatant to a final concentration of 20 mM. The solution was incubated at 4 ^{o}C for two days before centrifugation at 4,000 xg for 15 min to compress the fibrin gel. The supernatant was then collected for cell culture.[121]

B) Sterile calcium chloride (1 M in deionized water) was added to the platelet lysate supernatant to a final concentration of 20 mM. The solution was gently mixed by hand and incubated at room temperature for 4 hours, 4 ^{o}C for 12-16 hours, and 37 ^{o}C for 1 hour to induce fibrinogen polymerization and clot stabilization. The fibrin clot was mechanically disrupted before centrifugation at 3,000 xg for 20 minutes to pellet the gel fragments. The remaining supernatant was collected and added to cell culture media.[63]

C) The supernatant collected after two freeze-thaw cycles was diluted directly with cell culture medium to the desired final concentration. The solution was then mixed and incubated according to the protocol in procedure B to produce a fibrin gel. The fibrin gel was disrupted using mechanical agitation before centrifugation at 3,000 xg and filtration of the final supernatant through a 0.2 μm filter. The filtered supernatant was used directly for cell culture.[63]

The percent recovery of hPL using each protocol was calculated by dividing the final volume of recovered supernatant by the initial volume used for production.

3.2.2 Cell Culture

BM-hMSCs were purchased from the Institute for Regenerative Medicine (IRM, Texas A&M University), and cells between passages 3 and 6 were used for experiments. ihMSCs were produced according to a previously established protocol, and cells between passages 3 and 6 were used for experiments.[13] Cells were seeded at 1,000 (BM-MSC) or 500 (ihMSC) cells/cm^2 and expanded in CCM containing indicated concentrations of hPL or FBS (Atlanta Biologicals). Culture media was changed every 2 days until cells reached 70-80% confluence, at which point cells were harvested by exposure to 0.25% trypsin, 0.1% EDTA (Corning) for 5 minutes at 37 ^oC. After trypsin deactivation with CCM, cells were collected after centrifugation at 500 xg for 5 minutes and used for subsequent experiments.

Microcarrier culture was performed with ihMSCs seeded onto 25 cm^2 Synthemax™ II microcarriers (Corning) in low-attachment 6-well plates (Corning). After adjusting the media volume to 5 mL using CCM supplemented with either FBS or hPL, the cultures were incubated at 37 ^oC with agitation from a unidimensional rocker set to 6 RPM (Mimetas™). Media was exchanged every 2 days, and cells were recovered on days 6 and 8 using trypsin-EDTA, passed through a 40 μm cell strainer, and counted using hemocytometry.

3.2.3 Osteogenic Differentiation Assays

Osteogenic differentiation was performed as previously described.[87,89] Briefly, cells were seeded in 12-well plates and expanded to 70-80% confluence in CCM before replacing media with osteogenic basal medium (OBM) containing either hPL or FBS. In some experiments, 100 nM dexamethasone was added to OBM to be promote mineralization in differentiation cultures. Media was exchanged every 2 days until analysis via ARS according to the protocol in Chapter 2. Alkaline phosphatase (ALP) activity assays were performed as previously described.[89] Briefly, cells were washed and incubated at room temperature with p-Nitrophenyl Phosphate (PNPP, Sigma). Absorbance at 405 nm was recorded every 30 seconds, and the slope of absorbance change at 405 nm was determined and normalized to cell number using hemocytometry. Gene expression was analyzed using qRT-PCR after RNA extraction.

3.2.4 Adipogenic Differentiation Assays

Adipogenic differentiation was performed as previously described.[122] Briefly, cells were seeded in 12-well plates and expanded in CCM. Upon reaching 70-80% confluence, media was replaced with adipogenic differentiation medium (ADM) containing CCM, 500 nM dexamethasone (Sigma), 500 nM 3-isobutylmethylxanthine (Sigma), and 500 nM indomethacin (Sigma) for BM-MSC culture or CCM, 500 nM dexamethasone, 500 nM 3-isobutylmethylxanthine, and 50 µM indomethacin for ihMSC culture. Cultures were performed for 19 days with BM-MSC or 14 days with ihMSC with media exchanges every 2 days. In some experiments, ADM was supplemented with 10 µM troglitazone to enhance adipogenic differentiation.[123] After differentiation, cells

were washed with PBS and fixed with 4% (w/v) PFA in PBS for 15 minutes. After fixation, monolayers were washed with PBS and stained with freshly prepared 0.6% (w/v) ORO in 60% (v/v) isopropanol/40% (v/v) 1X PBS for 30 minutes. Monolayers were washed four times with PBS and imaged using bright field microscopy. Quantification of incorporated dye was performed using absorbance at 510 nm after dye extraction with 2% (w/v) sodium dodecyl sulfate (SDS) in 50% (v/v) ethanol/50% (v/v) 1X PBS for 20 minutes at room temperature. Additionally, gene expression was analyzed using qRT-PCR after RNA extraction.

3.2.5 Colony Forming Unit Assay

One hundred cells were seeded onto 15 cm dishes (Corning) in 25 mL CCM with 20% (v/v) FBS and incubated in a 37 ^{o}C, 5% CO_2 environment for 21 days. Cells were then stained and analyzed according to the protocol in Chapter 2.

3.2.6 RNA Extraction and qPCR

Total RNA was extracted from monolayers using a Qiagen RNeasy™ mini kit (Qiagen). Complimentary DNA (cDNA) was synthesized using a Superscript® III First-Strand Synthesis Kit according to the manufacturer's protocol, except for the use of a mixture of 50% random hexamer and 50% oligo-dT primers as previously described (Life Technologies).[123] Detection of PCR products was performed using SYBR-Green® assays (Applied Biosystems) on an AriaMx thermocycler (Agilent Technologies). Fold changed were determined using the $2^{-\Delta\Delta CT}$ method. Primer sequences used in this study are provided in Table 2.

3.2.7 Morphology Analysis

ihMSCs were seeded in 6-well plates (Corning) and expanded for 3 days before exposure to 10 μM CellTracker™ Green (Invitrogen) in serum-free CCM for 30 minutes at 37 ^{o}C. Cell monolayers were fixed with 4% paraformaldehyde in phosphate buffered saline (PBS) at room temperature for 15 minutes and incubated with 5 μg/mL Hoescht 33842 (Sigma-Aldrich) for 15 minutes. Images of cells were acquired using an Axio Vert.A1 fluorescent microscope (Zeiss). Captured images were analyzed according using CellProfiler using a modification of a previously established protocol.[124]

3.2.8 EV Production and Immunomodulation

EV production and immunomodulatory assays were performed as described in Chapter 2.

3.3 Results

3.3.1 Optimizing hPL Production as a Cell Culture Supplement

A set of experiments was performed with hPL purification techniques to determine which produced the most supplement from a given volume of platelets. A diagram of all media production techniques and yields is shown in Figure 3-1. All three techniques were cGMP-compatible and did not require the use of xenogeneic products during preparation and supplementation. However, the percent recovery of hPL significantly reduced when the fibrin polymer was not mechanically disrupted, with 80% of apheresis-derived hPL and 25% of random unit hPL volume purified for use. The protocols that involved disrupting the fibrin clot both led to recovery of approximately 90% of the initial hPL volume, regardless of platelet source. Preliminary experiments

were performed with the protocol listed in Figure 3-1 C, as it did not require the use of calcium chloride or other exogenous agents.

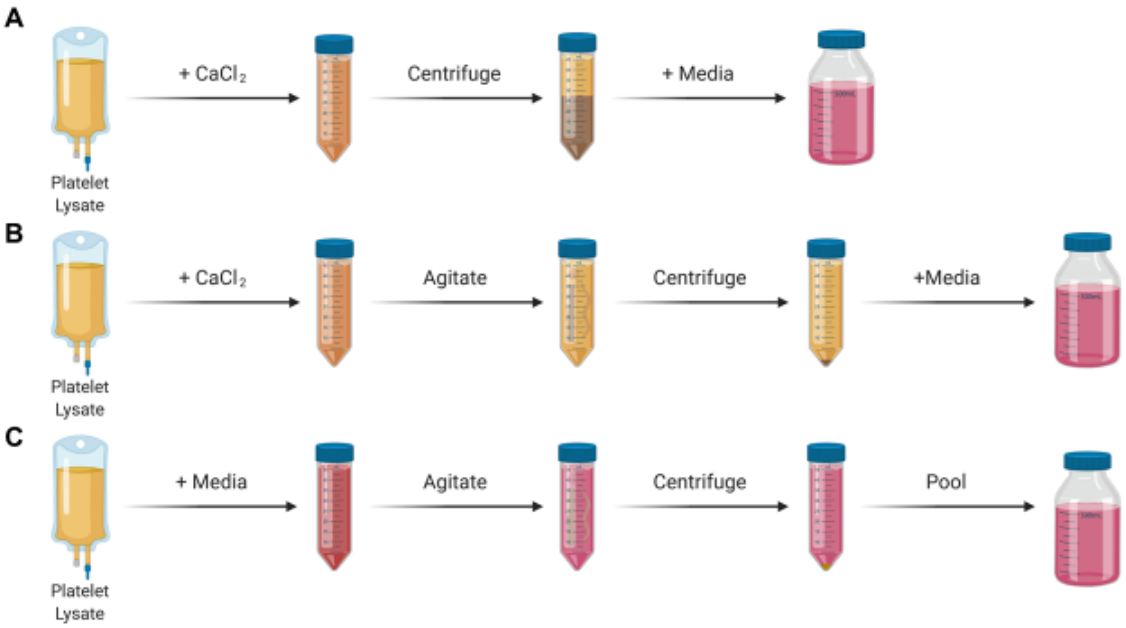

Preparation Protocol	A		B	C
	Apheresis	Random Unit		
Percent Recovery	80%	25%	90%	90%

Figure 3-1: Summary of Production Techniques for Different hPL Purification Protocols
A summary illustration of each protocol described in Methods section 3.2.1 is displayed in the figure above, with the letter to the left of each illustration corresponding to the protocol listed in the Methods section. The volume of liquid material recovered after fibrin removal are listed in the table.

3.3.2 Determining BM-hMSC Expansion and Differentiation in cGMP-Compliant hPL Culture

Media containing 10% or 5% (v/v) hPL, was used to expand and differentiate BM-hMSCs along osteogenic and adipogenic lineages. The doubling time of BM-

hMSCs was equivalent between FBS and both hPL concentrations (Figure 3-2 A). Mineralization after 21 days was completely inhibited after BM-hMSCs were expanded and differentiated in hPL. A small but statistically insignificant amount of ARS was observed in BM-hMSCs expanded in hPL and differentiated in FBS. Robust mineralization was observed in BM-hMSCs expanded and differentiated in FBS (Figure 3-2 B-C). Lipid droplet formation after expansion and differentiation in hPL was increased compared to the cells without differentiation or the cells differentiated in FBS. After differentiation in FBS-supplemented ADM, BM-hMSCs expanded in hPL had increased levels of lipid droplets compared to those expanded in FBS (Figure 3-2 D-E). Due to the absence of mineralization observed during osteogenic differentiation, chondrogenic differentiation was not performed on BM-hMSCs before transitioning to ihMSC culture.

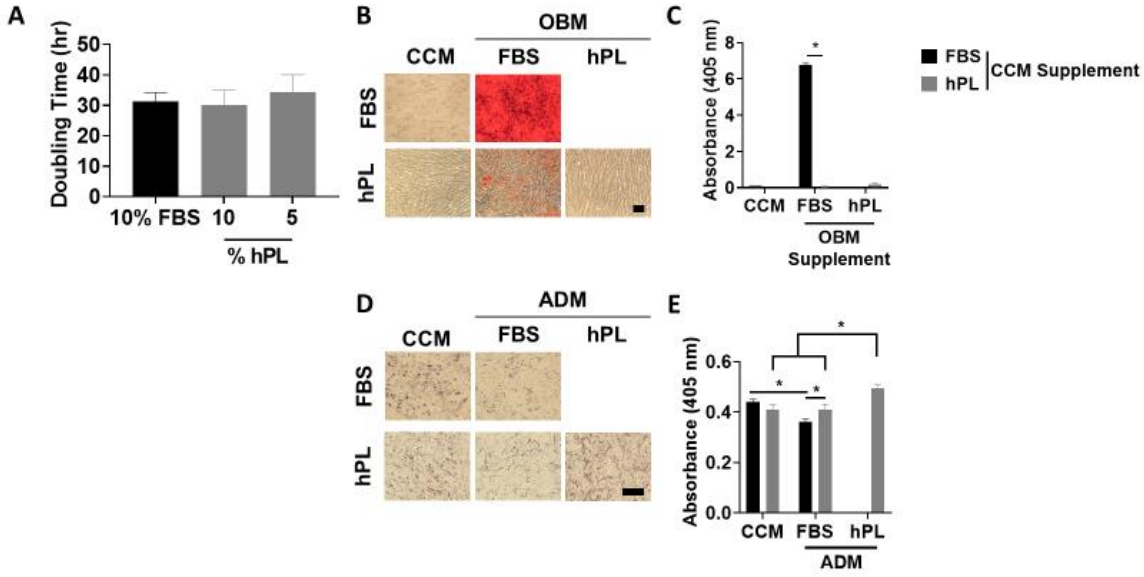

Figure 3-2: hPL Alters the Expansion and Osteogenic Differentiation of BM-hMSCs

(A) The doubling time of BM-hMSCs was not affected by hPL supplementation. (B) Alizarin Red S stained monolayers after osteogenic differentiation of BM-hMSCs demonstrated that expansion with 10% (v/v) hPL reduced osteogenic differentiation potential, even if differentiation is performed in OBM with FBS. (C) Quantification of Alizarin Red S extracts reflected the staining results. (D) Oil Red O stained monolayers after adipogenic differentiation of BM-hMSCs demonstrated higher amounts of Oil Red O droplets after expansion and differentiation in hPL. (E) Quantification of Oil Red O extracts confirmed this observation. Additionally, FBS supplementation reduced Oil Red deposition after expansion in FBS or hPL, though hPL expanded cells had higher levels of Oil Red O comparable to controls. Differences between media supplementation in (A) and (E) were analyzed using one-way ANOVA with Tukey's multiple comparison test and indicated by brackets, while differences between supplements in (C) and (E) were determined using two-tailed t-tests. * indicates statistical significance at $p<0.05$. Scale bar represents 100 µm.

3.3.3 Determining Optimal hPL Concentrations for ihMSC Culture Using Media

Trilineage differentiation, morphologic analysis, and immunomodulatory potential of ihMSCs were performed with lab-derived hPL prepared using exogenous calcium chloride and fibrin polymer disruption, as this technique uses cGMP-compliant ingredients and has been shown in previous studies to increase the calcium concentration

of cell culture media and enhance the mineralization potential of hMSCs.[63,125,126] Additionally, hPL supplementation at 5% (v/v) or lower was studied in ihMSC expansion due to the similarities observed between 10% and 5% during BM-hMSC culture. The doubling time and colony forming capabilities of ihMSCs were not significantly different when cultured in FBS and compared to any of the hPL concentrations tested (Figure 3-3 A-C). However, cells cultured in media supplemented with 2.5% hPL had a significantly reduced doubling time compared to those cultured in 1% hPL (Figure 3-3 A). Though there was no significant difference in the colony forming capabilities of the four culture conditions, ihMSCs isolated from 1% hPL cultures formed smaller, lighter colonies than those observed in the other conditions (Figure 3-3 B-C). Based on these results, expansion media used in subsequent experiments contained 2.5% hPL.

Quantification of ihMSC morphologic features using CellProfiler demonstrated that cells were smaller, less elongated, and had higher nucleus-to-cytoplasm area ratios after expansion in 2.5 % hPL relative to cells cultured with FBS. The morphologic features associated with hPL expansion is consistent with patterns typically associated with self-renewing MSCs (Figure 3-3 D-E). Finally, to determine whether 2.5% hPL supplementation affected 3-D microcarrier culture, ihMSCs were seeded onto Synthemax™ II microcarriers in low attachments with FBS or hPL supplementation. The expansion potential of ihMSCs on Synthemax™ II microcarriers in low attachment plates was equivalent between FBS- and hPL-supplemented cultures (Figure 3-3 F).

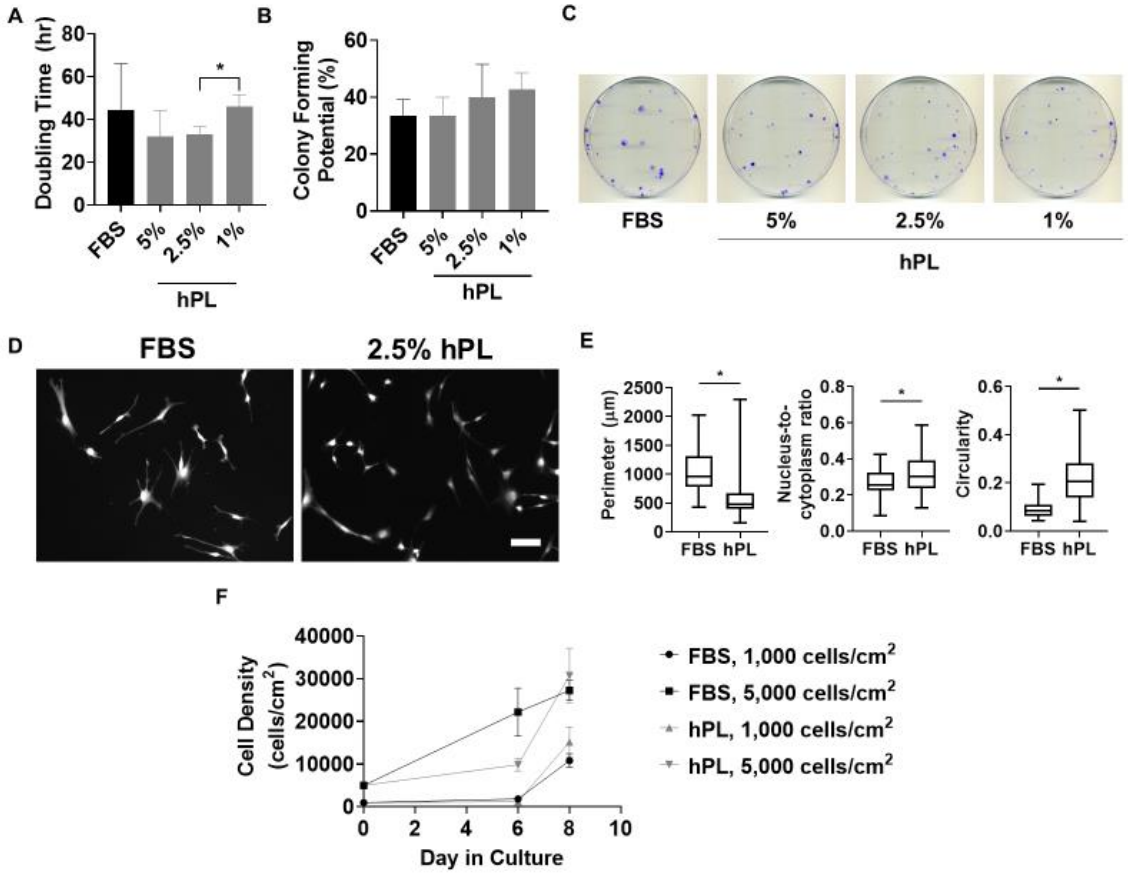

Figure 3-3: Supplementation with 2.5% hPL Supplemented Media Alters the Morphology but not the Expansion Potential of ihMSCs

(A) Population doubling times after 6 days of expansion were only different in ihMSC cultures containing 2.5% and 1% hPL. (B) ihMSCs expanded in FBS or hPL had comparable colony forming capabilities. (C) Representative images of colony forming unit plates used to generate the data shown in (B). (D) Representative images of cells expanded in FBS or hPL stained with CellTracker. (E) Quantification of cell shape parameters are shown in (E). (F) Expansion curves of ihMSCs on Corning Synthemax II microcarriers in low attachment plates demonstrated no significant difference in the expansion capabilities of cells grown in FBS or hPL. Differences in (A), (B), and the cell densities at day 8 in (E) were evaluated using one-way ANOVA with Tukey's multiple comparisons test. Differences in (C) and (D) were evaluated using a Mann-Whitney U test. * indicates statistically significant differences ($p<0.05$). Scale bar represents 100 μm.

3.3.4 Trilineage Differentiation Potential in hPL-Containing Media

Trilineage differentiation potential of ihMSCs was evaluated in both hPL- and FBS-supplemented media to determine if changes in osteogenic and adipogenic differentiation were similar to results presented in Figure 3-2 with BM-hMSC cultures. ihMSCs were cultured in osteogenic basal media (OBM) containing either FBS or hPL with or without dexamethasone (OBM+Dex) based off previous studies that indicate dexamethasone stimulates osteogenic differentiation.[109] Cells cultured in OBM containing FBS showed more intense ARS staining than cells cultured in OBM containing hPL (Figure 3-4 A), with the extent of staining quantified by absorbance. Adding dexamethasone nullified the differences in mineralization observed in OBM+Dex cultures containing FBS or hPL (Figure 3-4 A-B). In contrast to the decreased mineralization in OBM with hPL compared to OBM with FBS, ALP activity, an early marker of osteogenic differentiation, was higher on day 8 in OBM cultures containing hPL (Figure 3-4 C).

The expression of early and late osteogenic differentiation markers were evaluated on day 21 of culture to determine if any were changed with hPL supplementation.[109] Early markers of osteogenic differentiation, Runt-related transcription factor-2 (RUNX2), ALP, and late marker Osteocalcin (OCN) were not significantly different between CCM and OBM+Dex. Collagen type 1 alpha-1 (COLI) expression was increased in cultures containing hPL (Figure 3-4 D).

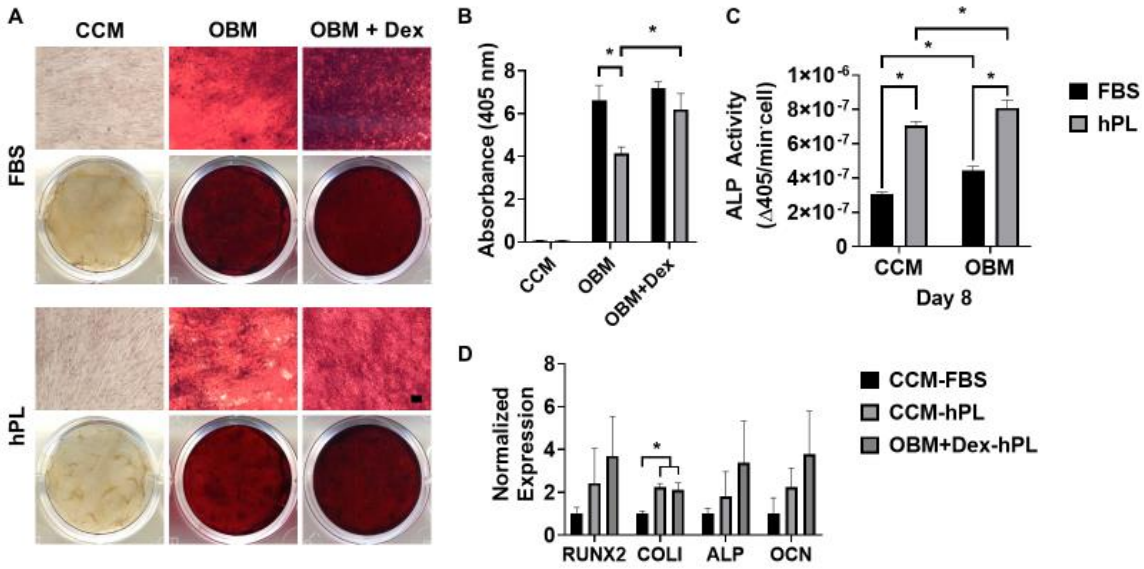

Figure 3-4: Osteogenic Differentiation Potential is Modulated by Supplementation of Culture Medium with hPL
(A) ARS staining of ihMSCs cultured in osteogenic medium (OBM) with or without dexamethasone demonstrated robust mineralization in all conditions, with cells in FBS mineralizing to a higher degree than those in hPL without dexamethasone administration. (B) Quantification of ARS staining confirmed the observations in (A). (C) ALP activity assays following 8 days of differentiation demonstrated significantly greater activity in ihMSCs cultured in hPL compared to FBS. (D) qRT-PCR analysis of osteogenic markers demonstrated significant increase in COLI expression with hPL treatment. Data is representative of three independent experiments. Differences in (A) and (C) were measured using two-tailed t-tests, and differences in (D) were analyzed using one-way ANOVA with Tukey's multiple comparisons test. Scale bar represents 100 µm. * represents significant difference ($p<0.05$).

After culture in adipogenic differentiation media, the number of ORO droplets was higher in hPL-supplemented cultures than those in FBS, with the differences confirmed by absorbance (Figure 3-5 A-B). When troglitazone was added to differentiation medium to further stimulate adipogenic differentiation, the ORO droplet number and size increased in both hPL- and FBS- supplemented ihMSC cultures, though the difference was not reflected in the absorbance values (Figure 3-5 A-B).

Gene expression for adipogenic markers was performed after 21 days of differentiation.[109] Peroxisome Proliferation-Activated Receptor-γ (PPARγ) expression was upregulated in response to ADM with FBS and ADM containing troglitazone with hPL (Figure 3-5 C). Expression of PPAR-γ was also higher in troglitazone cultures supplemented with hPL vs. FBS. The expression of Fatty Acid Binding Protein 4 (FAPB4), a late adipogenic marker, was only detected in ADM samples, but there was a significant increase in expression with both troglitazone and hPL supplementation (Figure 3-5 D). The expression of Lipoprotein Lipase (LPL), an early adipogenic marker, was not detectable in any sample except hPL-supplemented ADM treated with troglitazone (data not shown).

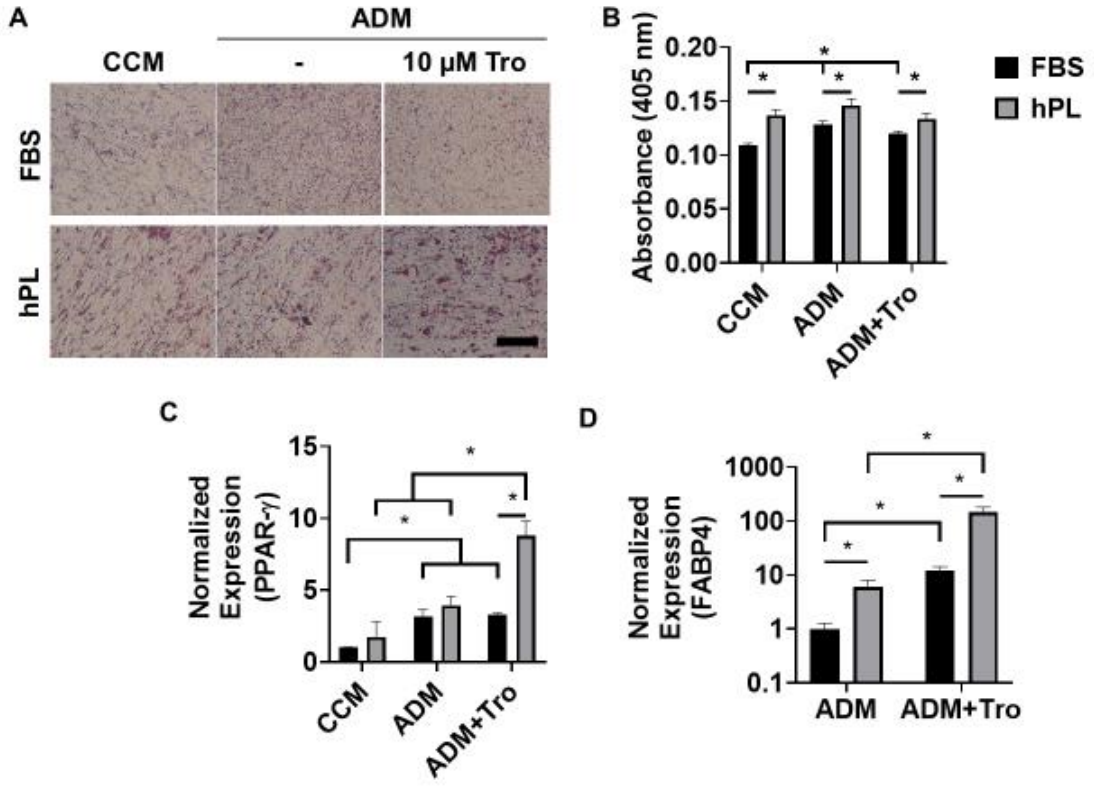

Figure 3-5: Adipogenic Differentiation is Enhanced with hPL Culture
(A) ORO staining of ihMSCs cultured in ADM with or without troglitazone demonstrated lipid accumulation in hPL-supplemented conditions. (B) Quantification of extracted ORO dye demonstrated higher amounts of dye recovered with hPL in each media condition, and a significant difference between every FBS condition. (C) qRT-PCR of PPAR-γ expression demonstrated upregulation of expression with ADM in FBS and troglitazone treatment in hPL supplemented media. (D) qRT-PCR of FABP4 expression demonstrated increased expression with troglitazone and hPL treatment. Data are representative of three independent experiments. Data in (B) and (C) were analyzed between media conditions using one-way ANOVA with Tukey's multiple comparisons test and between FBS and hPL with two-tailed t-tests. Data in (D) were analyzed using two-tailed t-tests. * represents significant difference between values ($p<0.05$). Scale bar represents 100 μm.

Finally, chondrogenic staining demonstrated increased Toluidine Blue staining after CDM treatment (Figure 3-6).

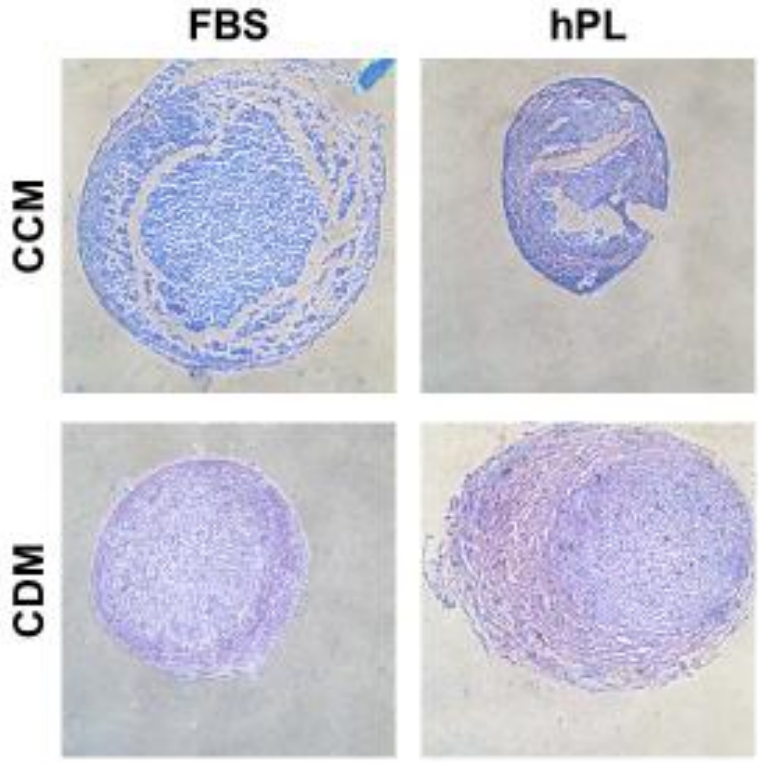

Figure 3-6: Chondrogenic Staining is Comparable Between both FBS and hPL Staining of ihMSC pellets with Toluidine Blue staining in CDM cultures indicates increased levels of proteoglycans compared to CCM cultures. Additionally, chondrocytes and lacunae are observed in CDM pellets.

3.3.5 ihMSC-Mediated Immunomodulation is Preserved after hPL Expansion

The immunomodulatory potential of ihMSCs after expansion in hPL or FBS was measured in splenocyte co-culture after stimulation with LPS. IL-6 secretion was suppressed by all doses from ihMSCs expanded in FBS and hPL (Figure 3-7 A). ihMSCs also inhibited IFN-γ secretion in a dose-dependent manner (Figure 3-7 B). Finally, TNF-α secretion was inhibited in all treatments, while only the FBS expanded ihMSCs were able to suppress the secretion in a dose-dependent manner (Figure 3-7 C). ihMSCs expanded in FBS were more potent than ihMSCs expanded in hPL at the 1:50 ratio.

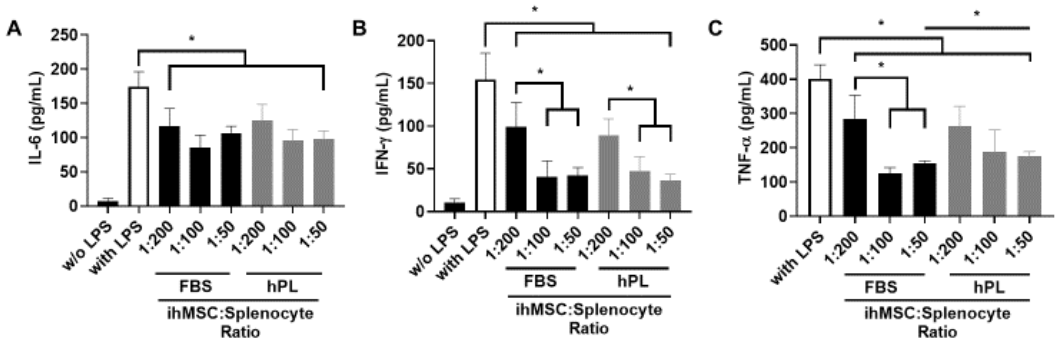

Figure 3-7: ihMSCs Expanded in hPL Retain the Ability to Suppress Cytokine Secretion

(A) IL-6 ELISA demonstrated that all ihMSC treatments were able to suppress IL-6. (B) IFN-γ ELISA demonstrated that all ihMSC groups were able to suppress IFN-γ in a dose-dependent manner. (C) TNF-α ELISA demonstrated that all ihMSC groups suppressed TNF-α secretion, and FBS suppressed secretion in a dose-dependent manner. Differences between positive control and all treatments were determined using one-way ANOVA with Dunnett's multiple comparisons test. Differences between all doses from a specific media supplement were determined using one-way ANOVA with Tukey's multiple comparison test. Differences between FBS and hPL at specific ihMSC:splenocyte ratios were determined using two-tailed t-tests. * indicates significant difference at $p<0.05$.

3.3.6 EV Production and Immunomodulation After hPL Expansion

To determine whether EVs isolated from hPL-expanded cells had immunomodulatory potential, purified EVs were characterized and used in the LPS-stimulated splenocyte activation model. The number of EVs isolated from hPL cultures was increased compared to FBS cultures, though there were not enough replicates tested to determine statistical significance (Figure 3-8 A). Additionally, the number of secreted EVs per cell was higher after ihMSC expansion in hPL (Figure 3-8 B). The average diameter of both EV populations was similar, and histograms of both populations were within the diameter range of exosomes (Figure 3-8 C). The collected EVs from media supplemented with either hPL or FBS did not suppress the secretion of IL-6, though one

dose from FBS-expanded cells did suppress IFN-γ (Figure 3-8 D-E). However, this pattern was not reproducible in a dose-dependent manner.

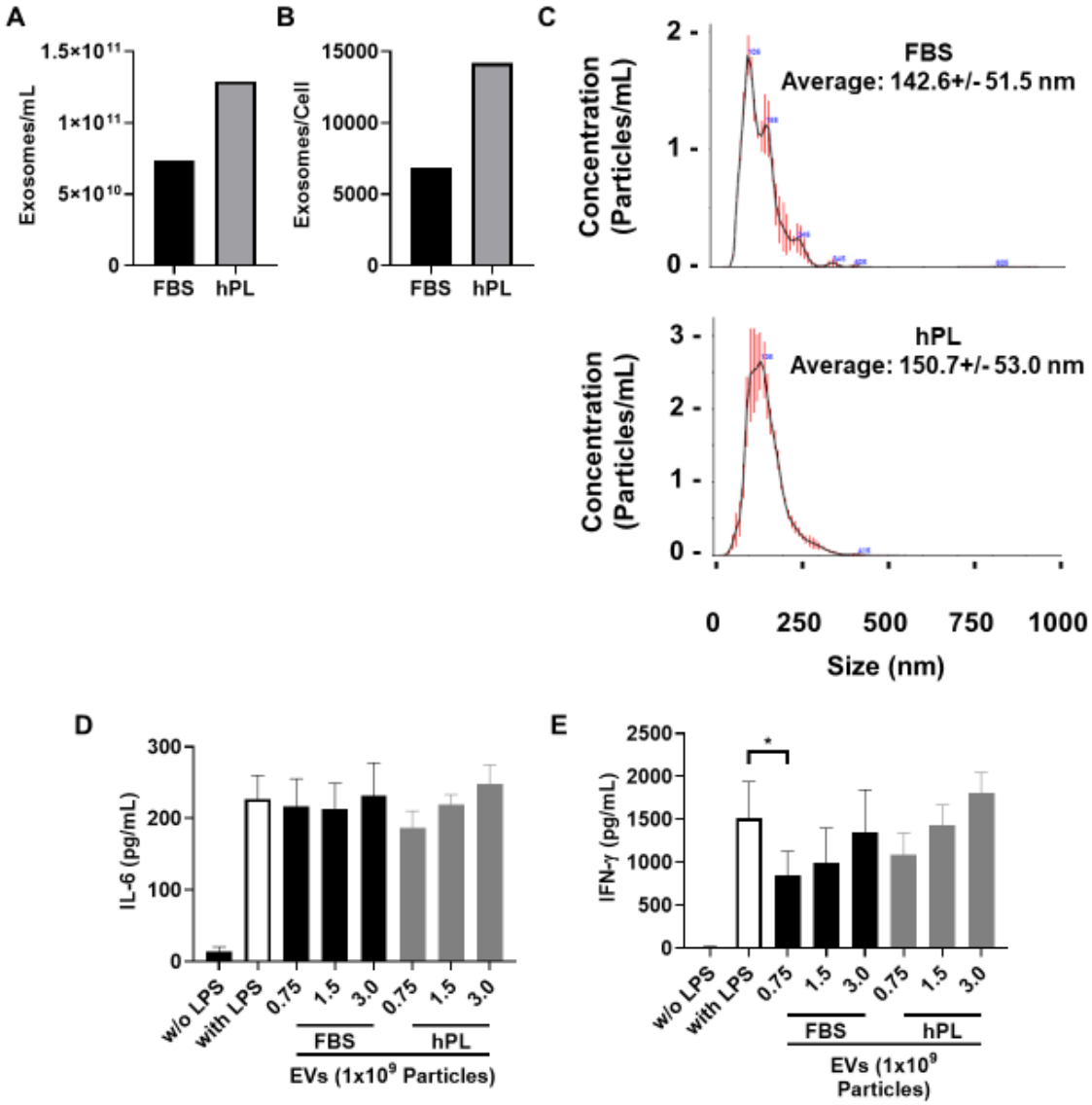

Figure 3-8: hPL-Expanded ihMSCs Produce Increased Numbers of EVs That Are Not Immunomodulatory

(A) Quantification of the EV concentration revealed higher numbers of EVs after hPL expansion. (B) Normalization of EV number by cell counts demonstrated that hPL-expanded ihMSCs secreted more EVs over 24 hours than FBS-expanded ihMSCs. (C) Diameter histograms of recovered EVs were of similar diameter. (D) IL-6 ELISA demonstrated no EV dose suppressed secretion. (E) IFN-γ secretion was lowered in one

dose of FBS EVs, though the effect was not dose-dependent. The differences between positive control and EV doses in (D) and (E) were determined using one-way ANOVA with Dunnet's multiple comparisons test. * indicates significant difference at $p<0.05$.

3.4 Discussion

In this study, we explored the expansion capability and phenotypic changes of BM-hMSCs and ihMSCs after transitioning them to animal-free cell culture with hPL. We observed that both BM-hMSCs and ihMSCs had the same expansion capabilities and colony forming potential regardless of culture in hPL or FBS. Additionally, hPL supported the expansion of ihMSCs on microcarrier surfaces in low-attachment well plates. hPL supplementation inhibited mineralization in both BM-hMSC and ihMSC cultures without the use of dexamethasone. In contrast, adipogenic differentiation was induced with hPL supplementation in both cell types. The immunomodulation potential of ihMSCs was preserved after hPL expansion, and production of EVs was elevated compared to FBS, though the EVs lacked immunomodulatory potential. Taken together, we have observed that culture of BM-hMSCs and ihMSCs with hPL impacts differentiation potential but preserves expansion capabilities and cellular immunomodulatory potential.

Initial experiments were performed with BM-hMSCs and hPL-supplemented media prepared without exogenous calcium chloride addition because previous studies demonstrated equal expansion and differentiation potential for MSCs cultured in hPL or FBS.[63] Though expansion was preserved during culture with BM-hMSCs, the improved adipogenic but inhibited osteogenic differentiation led us to pursue other hPL purification protocols. We therefore used purification protocols that used calcium

chloride. Additionally, previous studies had demonstrated higher calcium concentrations in cell culture medium after hPL preparation with exogenous calcium chloride.[125] ihMSCs were also used in further experiments instead of BM-hMSCs due to their enhanced osteogenic differentiation potential and potential for limited donor variability.[123]

Mineralization was observed in ihMSCs with hPL-supplemented OBM, though the degree of mineralization was equal to FBS only when dexamethasone was added. Additionally, osteogenic gene expression was not enhanced in hPL-supplemented cultures even with dexamethasone. Dexamethasone is a typical component of osteogenic differentiation media for the activation of Runx2-dependent transcription.[109] Though the molecular mechanisms behind our observations are unknown, differences in growth factor concentrations between FBS and hPL could modulate other signaling pathways involved in osteogenic differentiation and ALP production.[109] The concentration of soluble factors in hPL could also explain the differences observed in lipid droplet accumulation and gene expression observed during adipogenic differentiation. Future experiments including signaling pathway analysis may further define which ihMSC molecular processes are affected by hPL supplementation.

Chondrogenic differentiation was observed in both hPL and FBS-treated cells. Though the comparisons were only made using microscopy, future experiments including the evaluation of chondrogenic gene expression and the measurement of sulfated glycosaminoglycans could further delineate any differences in chondrogenic differentiation potential.[109,127]

There is debate whether hPL supplementation preserves or suppresses hMSC immunomodulatory potential.[115,116,118,128,129] Our study supports the evidence that hMSC immunomodulatory potential is preserved after hPL supplementation. The immunomodulatory potential of EVs isolated from chemically-defined CDPF media has not been evaluated after hPL expansion, though previous studies have demonstrated that EVs recovered after FBS supplementation reduce cytokine secretion after LPS stimulation in murine splenocytes.[25,80] Our studies showed that ihMSCs expanded in hPL were capable of producing higher numbers of EVs compared to FBS. However, neither FBS- nor hPL-derived EVs suppressed cytokine secretion following LPS stimulation. CDPF has been shown to induce a stress response in hMSCs for 6 hours after initial exposure, thereby affecting the produced EVs during that time.[91] Previous studies have exchanged CDPF media 6 hours after initial exposure, while the protocol used in our study did not.[91] Subsequent experiments could be performed using the previously published protocols to further characterize the EV immunomodulatory potential. Additionally, the recovered EVs could be used in other *in vitro* inflammatory assays that model other disease conditions such as GvHD.[110]

In conclusion, we have demonstrated that xeno-free media prepared using previously published protocols supports the expansion, differentiation, and immunomodulatory potential of ihMSCs. We have also demonstrated that expansion is preserved in BM-hMSC culture but osteogenic differentiation is not. This data provides a basis for further characterization of hPL on immunomodulatory capabilities of ihMSCs

and their EVs, and the transition of microcarrier culture from low-attachment well plates to bioreactors.

CHAPTER 4

CONCLUSIONS

4.1 Summary of Thesis and Future Work

Despite the success of hMSC-derived therapies to treat inflammatory diseases in pre-clinical and clinical trials, monolayer methods will not be able to meet demand should these treatments become FDA approved. Efforts to produce hMSCs have used xenobiotic reagents, and have relied on monolayer culture in cell stacks or multilayer culture vessels. The FDA has provided guidance against the use of xenogenic agents to produce human therapeutics, and cell recovery from monolayers are cumbersome and do not lead to complete recovery. The work presented in this dissertation presents systematic techniques to explore the production of materials for hMSC expansion in scalable bioreactors.

In Chapter 2, ihMSCs were expanded on GelMA microcarriers in two types of bioreactors while preserving clonogenic, differentiation, and immunomodulatory potential. The optimal GelMA microcarrier generation production technique was determined to be step emulsification via recovered microcarrier conditions such as diameter variability and cost analyses. Of the two GelMA weight percentages used in this study, 15-fold expansion of ihMSCs was achieved after seeding at 1,000 cells/cm^2 using low attachment well plates, though 7.5% GelMA microcarriers were the only substrate comparable to commercialy-available microcarriers. Bioreactor expanded ihMSCs retained clonogenic and differentiation potential but developed improved immunomodulatory potential after RWVB expansion. Additionally, we demonstrated

that EVs harvested after bioreactor culture were capable of suppressing cytokine secretion after leukocyte activation. Without optimization of cell culture conditions, current bioreactor culture generates 75,000 cells/mL after 8 days of expansion. If directly scaled to 80 L, this cell expansion can generate 6 billion ihMSCs enough for the treatment of 7 50 kg patients with SR-aGvHD. Previous studies have found that optimized vertical wheel bioreactors support hMSC expansion to 300,000 cells/mL, increasing the number of treatments to 30.[71,99]

In Chapter 3, we determined that two cGMP-compatible hPL production techniques lead to 90% recovery of the initial platelet unit. These hPL preparations supported similar population doubling times compared to FBS supplemented cultures while promoting morphologic features of self-renewing cells. hPL supplementation reduced osteogenic differentiation of both BM-hMSCs and ihMSCs while improving adipogenic differentiation potential and maintaining chondrogenic potential. Finally, we demonstrated that ihMSCs expanded in hPL retained immunomodulatory capabilities, demonstrating that ihMSCs can be cultured in xeno-free culture conditions for therapeutic applications.

Future work will focus on scaling cell expansion on GelMA microcarriers and incorporating hPL into bioreactor cell culture. The production of GelMA microcarriers and the expansion of ihMSCs in bioreactors with hPL-supplemented media can be optimized to maximize production in multiliter vertical wheel bioreactors. Finally, isolated ihMSCs and EVs can be used for treating inflammatory conditions in animal models with an eye towards producing therapeutic grade cells for human therapeutics.

REFERENCES

1 Jacobsohn, D. A. & Vogelsang, G. B. Acute graft versus host disease. *Orphanet J Rare Dis* **2**, 35, doi:10.1186/1750-1172-2-35 (2007).

2 Le Blanc, K. *et al.* Mesenchymal stem cells for treatment of steroid-resistant, severe, acute graft-versus-host disease: a phase II study. *Lancet (London, England)* **371**, 1579-1586, doi:10.1016/S0140-6736(08)60690-X (2008).

3 Vaillant, A. J. & Mohammadi, O. *Graft Versus Host Disease*, <https://www.ncbi.nlm.nih.gov/books/NBK538235/> (2022).

4 Galleu, A. *et al.* Mesenchymal stromal cells for acute graft-versus-host disease: response at 1 week predicts probability of survival. *British journal of haematology* **185**, 89-92, doi:10.1111/bjh.15749 (2019).

5 Cahn, J. Y. *et al.* Prospective evaluation of 2 acute graft-versus-host (GVHD) grading systems: a joint Societe Francaise de Greffe de Moelle et Therapie Cellulaire (SFGM-TC), Dana Farber Cancer Institute (DFCI), and International Bone Marrow Transplant Registry (IBMTR) prospective study. *Blood* **106**, 1495-1500, doi:10.1182/blood-2004-11-4557 (2005).

6 Galipeau, J. & Sensebe, L. Mesenchymal Stromal Cells: Clinical Challenges and Therapeutic Opportunities. *Cell Stem Cell* **22**, 824-833, doi:10.1016/j.stem.2018.05.004 (2018).

7 Ghoryani, M. *et al.* Amelioration of clinical symptoms of patients with refractory rheumatoid arthritis following treatment with autologous bone marrow-derived mesenchymal stem cells: A successful clinical trial in Iran. *Biomed Pharmacother* **109**, 1834-1840, doi:10.1016/j.biopha.2018.11.056 (2019).

8 Panes, J. *et al.* Expanded allogeneic adipose-derived mesenchymal stem cells (Cx601) for complex perianal fistulas in Crohn's disease: a phase 3 randomised, double-blind controlled trial. *Lancet (London, England)* **388**, 1281-1290, doi:10.1016/S0140-6736(16)31203-X (2016).

9 Kordelas, L. *et al.* MSC-derived exosomes: a novel tool to treat therapy-refractory graft-versus-host disease. *Leukemia* **28**, 970-973, doi:10.1038/leu.2014.41 (2014).

10 Olsen, T. R., Ng, K. S., Lock, L. T., Ahsan, T. & Rowley, J. A. Peak MSC-Are We There Yet? *Front Med (Lausanne)* **5**, 178, doi:10.3389/fmed.2018.00178 (2018).

11 Cheng, R. J. *et al.* Mesenchymal Stem Cells: Allogeneic MSC May Be Immunosuppressive but Autologous MSC Are Dysfunctional in Lupus Patients. *Front Cell Dev Biol* **7**, 285, doi:10.3389/fcell.2019.00285 (2019).

12 Jossen, V., van den Bos, C., Eibl, R. & Eibl, D. Manufacturing human mesenchymal stem cells at clinical scale: process and regulatory challenges. *Appl Microbiol Biotechnol* **102**, 3981-3994, doi:10.1007/s00253-018-8912-x (2018).

13 Zhao, Q. *et al.* MSCs derived from iPSCs with a modified protocol are tumor-tropic but have much less potential to promote tumors than bone marrow MSCs. *Proc Natl Acad Sci U S A* **112**, 530-535, doi:10.1073/pnas.1423008112 (2015).

14 Prockop, D. J. The exciting prospects of new therapies with mesenchymal stromal cells. *Cytotherapy* **19**, 1-8, doi:10.1016/j.jcyt.2016.09.008 (2017).

15 Kabat, M., Bobkov, I., Kumar, S. & Grumet, M. Trends in mesenchymal stem cell clinical trials 2004-2018: Is efficacy optimal in a narrow dose range? *Stem Cells Transl Med* **9**, 17-27, doi:10.1002/sctm.19-0202 (2020).

16 Pereira Chilima, T. D., Moncaubeig, F. & Farid, S. S. Impact of allogeneic stem cell manufacturing decisions on cost of goods, process robustness and reimbursement. *Biochemical Engineering Journal* **137**, 132-151, doi:10.1016/j.bej.2018.04.017 (2018).

17 Bandeiras, C., Cabral, J. M., Finkelstein, S. N. & Ferreira, F. C. Modeling biological and economic uncertainty on cell therapy manufacturing: the choice of culture media supplementation. *Regen Med* **13**, 917-933, doi:10.2217/rme-2018-0034 (2018).

18 Viau, S. *et al.* Pathogen reduction through additive-free short-wave UV light irradiation retains the optimal efficacy of human platelet lysate for the expansion of human bone marrow mesenchymal stem cells. *PLoS One* **12**, e0181406, doi:10.1371/journal.pone.0181406 (2017).

19 Friedenstein, A. J., Gorskaja, J. F. & Kulagina, N. N. Fibroblast precursors in normal and irradiated mouse hematopoietic organs. *Exp Hematol* **4**, 267-274 (1976).

20 Dominici, M. *et al.* Minimal criteria for defining multipotent mesenchymal stromal cells. The International Society for Cellular Therapy position statement. *Cytotherapy* **8**, 315-317, doi:10.1080/14653240600855905 (2006).

21 Negi, N. & Griffin, M. D. Effects of mesenchymal stromal cells on regulatory T cells: Current understanding and clinical relevance. *Stem Cells* **38**, 596-605, doi:10.1002/stem.3151 (2020).

22 Cosenza, S., Ruiz, M., Maumus, M., Jorgensen, C. & Noel, D. Pathogenic or Therapeutic Extracellular Vesicles in Rheumatic Diseases: Role of Mesenchymal Stem Cell-Derived Vesicles. *Int J Mol Sci* **18**, doi:10.3390/ijms18040889 (2017).

23 Witwer, K. W. *et al.* Defining mesenchymal stromal cell (MSC)-derived small extracellular vesicles for therapeutic applications. *J Extracell Vesicles* **8**, 1609206, doi:10.1080/20013078.2019.1609206 (2019).

24 Zhang, B. *et al.* Mesenchymal stem cells secrete immunologically active exosomes. *Stem Cells Dev* **23**, 1233-1244, doi:10.1089/scd.2013.0479 (2014).

25 Kim, H. *et al.* Comprehensive Molecular Profiles of Functionally Effective MSC-Derived Extracellular Vesicles in Immunomodulation. *Mol Ther* **28**, 1628-1644, doi:10.1016/j.ymthe.2020.04.020 (2020).

26 Hassan, M. *et al.* Large-Scale Expansion of Human Mesenchymal Stem Cells. *Stem Cells Int* **2020**, 9529465, doi:10.1155/2020/9529465 (2020).

27 Phinney, D. G., Galipeau, J., Msc Committee Of The International Society Of, C. & Gene, T. Manufacturing mesenchymal stromal cells for clinical applications: A survey of Good Manufacturing Practices at U.S. academic centers. *Cytotherapy* **21**, 782-792, doi:10.1016/j.jcyt.2019.04.003 (2019).

28 Bartosh, T. J. *et al.* Aggregation of human mesenchymal stromal cells (MSCs) into 3D spheroids enhances their antiinflammatory properties. *Proc Natl Acad Sci U S A* **107**, 13724-13729, doi:10.1073/pnas.1008117107 (2010).

29 Cabral, J. M., da Silva, C. L., Chase, L. G. & Diogo, M. M. *Stem Cell Manufacturing*. (Elsevier, 2016).

30 Tsai, A. C., Jeske, R., Chen, X., Yuan, X. & Li, Y. Influence of Microenvironment on Mesenchymal Stem Cell Therapeutic Potency: From Planar Culture to Microcarriers. *Front Bioeng Biotechnol* **8**, 640, doi:10.3389/fbioe.2020.00640 (2020).

31 Cunha, B. *et al.* Filtration methodologies for the clarification and concentration of human mesenchymal stem cells. *Journal of Membrane Science* **478**, 117-129, doi:10.1016/j.memsci.2014.12.041 (2015).

32 Jo, Y. K. & Lee, D. Biopolymer Microparticles Prepared by Microfluidics for Biomedical Applications. *Small* **16**, e1903736, doi:10.1002/smll.201903736 (2020).

33 Dosta, P. *et al.* Scale-up manufacturing of gelatin-based microcarriers for cell therapy. *J Biomed Mater Res B Appl Biomater* **108**, 2937-2949, doi:10.1002/jbm.b.34624 (2020).

34 Wissemann, K. W. & Jacobson, B. S. Pure gelatin microcarriers: synthesis and use in cell attachment and growth of fibroblast and endothelial cells. *In Vitro Cell Dev Biol* **21**, 391-401, doi:10.1007/BF02623470 (1985).

35 Yue, K. *et al.* Synthesis, properties, and biomedical applications of gelatin methacryloyl (GelMA) hydrogels. *Biomaterials* **73**, 254-271, doi:10.1016/j.biomaterials.2015.08.045 (2015).

36 Dong, Z. *et al.* Gelatin methacryloyl (GelMA)-based biomaterials for bone regeneration. *RSC Advances* **9**, 17737-17744, doi:10.1039/c9ra02695a (2019).

37 Pepelanova, I., Kruppa, K., Scheper, T. & Lavrentieva, A. Gelatin-Methacryloyl (GelMA) Hydrogels with Defined Degree of Functionalization as a Versatile Toolkit for 3D Cell Culture and Extrusion Bioprinting. *Bioengineering (Basel)* **5**, doi:10.3390/bioengineering5030055 (2018).

38 Sheikhi, A. *et al.* Microengineered Emulsion-to-Powder Technology for the High-Fidelity Preservation of Molecular, Colloidal, and Bulk Properties of Hydrogel Suspensions. *ACS Applied Polymer Materials* **1**, 1935-1941, doi:10.1021/acsapm.9b00265 (2019).

39 Zhao, X. *et al.* Injectable Stem Cell-Laden Photocrosslinkable Microspheres Fabricated Using Microfluidics for Rapid Generation of Osteogenic Tissue Constructs. *Advanced Functional Materials* **26**, 2809-2819, doi:10.1002/adfm.201504943 (2016).

40 Haliburton, J. R. *et al.* Efficient extraction of oil from droplet microfluidic emulsions. *Biomicrofluidics* **11**, 034111, doi:10.1063/1.4984035 (2017).

41 Guha, I. F. & Varanasi, K. K. Separating nanoscale emulsions: Progress and challenges to date. *Current Opinion in Colloid & Interface Science* **36**, 110-117, doi:10.1016/j.cocis.2018.02.001 (2018).

42 Sulaiman, S. *et al.* 3D Culture of MSCs on a Gelatin Microsphere in a Dynamic Culture System Enhances Chondrogenesis. *Int J Mol Sci* **21**, doi:10.3390/ijms21082688 (2020).

43 Nguyen, A. H., McKinney, J., Miller, T., Bongiorno, T. & McDevitt, T. C. Gelatin methacrylate microspheres for controlled growth factor release. *Acta Biomater* **13**, 101-110, doi:10.1016/j.actbio.2014.11.028 (2015).

44 Li, W. *et al.* Microfluidic fabrication of microparticles for biomedical applications. *Chem Soc Rev* **47**, 5646-5683, doi:10.1039/c7cs00263g (2018).

45 Montessori, A., Lauricella, M., Succi, S., Stolovicki, E. & Weitz, D. Elucidating the mechanism of step emulsification. *Physical Review Fluids* **3**, doi:10.1103/PhysRevFluids.3.072202 (2018).

46 Eggersdorfer, M. L., Seybold, H., Ofner, A., Weitz, D. A. & Studart, A. R. Wetting controls of droplet formation in step emulsification. *Proc Natl Acad Sci U S A* **115**, 9479-9484, doi:10.1073/pnas.1803644115 (2018).

47 Dangla, R., Fradet, E., Lopez, Y. & Baroud, C. N. The physical mechanisms of step emulsification. *Journal of Physics D: Applied Physics* **46**, 114003, doi:10.1088/0022-3727/46/11/114003 (2013).

48 Alimperti, S. *et al.* Serum-free spheroid suspension culture maintains mesenchymal stem cell proliferation and differentiation potential. *Biotechnol Prog* **30**, 974-983, doi:10.1002/btpr.1904 (2014).

49 Schallmoser, K. *et al.* Human platelet lysate can replace fetal bovine serum for clinical-scale expansion of functional mesenchymal stromal cells. *Transfusion* **47**, 1436-1446, doi:10.1111/j.1537-2995.2007.01220.x (2007).

50 Cherian, D. S., Bhuvan, T., Meagher, L. & Heng, T. S. P. Biological Considerations in Scaling Up Therapeutic Cell Manufacturing. *Front Pharmacol* **11**, 654, doi:10.3389/fphar.2020.00654 (2020).

51 Viau, S. *et al.* A highly standardized and characterized human platelet lysate for efficient and reproducible expansion of human bone marrow mesenchymal stromal cells. *Cytotherapy* **21**, 738-754, doi:10.1016/j.jcyt.2019.04.053 (2019).

52 Regulatory considerations for human cells, tissues, and cellular and tissue-based products: Minimal manipulation and homologous use. (US Food and Drug Administration, https://www.fda.gov/regulatory-information/search-fda-guidance-documents/regulatory-considerations-human-cells-tissues-and-cellular-and-tissue-based-products-minimal, 2020).

53 Bieback, K., Fernandez-Munoz, B., Pati, S. & Schafer, R. Gaps in the knowledge of human platelet lysate as a cell culture supplement for cell therapy: a joint publication from the AABB and the International Society for Cell & Gene Therapy. *Cytotherapy* **21**, 911-924, doi:10.1016/j.jcyt.2019.06.006 (2019).

54 Henschler, R., Gabriel, C., Schallmoser, K., Burnouf, T. & Koh, M. B. C. Human platelet lysate current standards and future developments. *Transfusion* **59**, 1407-1413, doi:10.1111/trf.15174 (2019).

55 Schallmoser, K., Henschler, R., Gabriel, C., Koh, M. B. C. & Burnouf, T. Production and Quality Requirements of Human Platelet Lysate: A Position Statement from the Working Party on Cellular Therapies of the International Society of Blood Transfusion. *Trends Biotechnol* **38**, 13-23, doi:10.1016/j.tibtech.2019.06.002 (2020).

56 Strunk, D. *et al.* International Forum on GMP-grade human platelet lysate for cell propagation. *Vox Sang* **113**, e1-e25, doi:10.1111/vox.12594 (2018).

57 Shih, D. T. & Burnouf, T. Preparation, quality criteria, and properties of human blood platelet lysate supplements for ex vivo stem cell expansion. *N Biotechnol* **32**, 199-211, doi:10.1016/j.nbt.2014.06.001 (2015).

58 Burnouf, T., Strunk, D., Koh, M. B. & Schallmoser, K. Human platelet lysate: Replacing fetal bovine serum as a gold standard for human cell propagation? *Biomaterials* **76**, 371-387, doi:10.1016/j.biomaterials.2015.10.065 (2016).

59 Becherucci, V. *et al.* Human platelet lysate in mesenchymal stromal cell expansion according to a GMP grade protocol: a cell factory experience. *Stem Cell Res Ther* **9**, 124, doi:10.1186/s13287-018-0863-8 (2018).

60 Gupta, P., Hall, G. N., Geris, L., Luyten, F. P. & Papantoniou, I. Human Platelet Lysate Improves Bone Forming Potential of Human Progenitor Cells Expanded in Microcarrier-Based Dynamic Culture. *Stem Cells Transl Med* **8**, 810-821, doi:10.1002/sctm.18-0216 (2019).

61 Boraldi, F., Burns, J. S., Bartolomeo, A., Dominici, M. & Quaglino, D. Mineralization by mesenchymal stromal cells is variously modulated depending on commercial platelet lysate preparations. *Cytotherapy* **20**, 335-342, doi:10.1016/j.jcyt.2017.11.011 (2018).

62 Copland, I. B., Garcia, M. A., Waller, E. K., Roback, J. D. & Galipeau, J. The effect of platelet lysate fibrinogen on the functionality of MSCs in immunotherapy. *Biomaterials* **34**, 7840-7850, doi:10.1016/j.biomaterials.2013.06.050 (2013).

63 Laner-Plamberger, S. *et al.* Mechanical fibrinogen-depletion supports heparin-free mesenchymal stem cell propagation in human platelet lysate. *J Transl Med* **13**, 354, doi:10.1186/s12967-015-0717-4 (2015).

64 Warnke, P. H. *et al.* A clinically-feasible protocol for using human platelet lysate and mesenchymal stem cells in regenerative therapies. *J Craniomaxillofac Surg* **41**, 153-161, doi:10.1016/j.jcms.2012.07.003 (2013).

65 Gyorgy, B., Hung, M. E., Breakefield, X. O. & Leonard, J. N. Therapeutic applications of extracellular vesicles: clinical promise and open questions. *Annual review of pharmacology and toxicology* **55**, 439-464, doi:10.1146/annurev-pharmtox-010814-124630 (2015).

66 Martin, I., Galipeau, J., Kessler, C., Le Blanc, K. & Dazzi, F. Challenges for mesenchymal stromal cell therapies. *Sci Transl Med* **11**, doi:10.1126/scitranslmed.aat2189 (2019).

67 Wiklander, O. P. B., Brennan, M. A., Lotvall, J., Breakefield, X. O. & El Andaloussi, S. Advances in therapeutic applications of extracellular vesicles. *Sci Transl Med* **11**, doi:10.1126/scitranslmed.aav8521 (2019).

68 Gowen, A., Shahjin, F., Chand, S., Odegaard, K. E. & Yelamanchili, S. V. Mesenchymal Stem Cell-Derived Extracellular Vesicles: Challenges in Clinical Applications. *Front Cell Dev Biol* **8**, 149, doi:10.3389/fcell.2020.00149 (2020).

69 Tavassoli, H. *et al.* Large-scale production of stem cells utilizing microcarriers: A biomaterials engineering perspective from academic research to commercialized products. *Biomaterials* **181**, 333-346, doi:10.1016/j.biomaterials.2018.07.016 (2018).

70 Mizukami, A. *et al.* Technologies for large-scale umbilical cord-derived MSC expansion: Experimental performance and cost of goods analysis. *Biochemical Engineering Journal* **135**, 36-48, doi:10.1016/j.bej.2018.02.018 (2018).

71 de Sousa Pinto, D. *et al.* Scalable Manufacturing of Human Mesenchymal Stromal Cells in the Vertical-Wheel Bioreactor System: An Experimental and Economic Approach. *Biotechnol J* **14**, e1800716, doi:10.1002/biot.201800716 (2019).

72 Simaria, A. S. *et al.* Allogeneic cell therapy bioprocess economics and optimization: single-use cell expansion technologies. *Biotechnology and bioengineering* **111**, 69-83, doi:10.1002/bit.25008 (2014).

73 Lawson, T. *et al.* Process development for expansion of human mesenchymal stromal cells in a 50L single-use stirred tank bioreactor. *Biochemical Engineering Journal* **120**, 49-62, doi:10.1016/j.bej.2016.11.020 (2017).

74 Haraszti, R. A. *et al.* Exosomes Produced from 3D Cultures of MSCs by Tangential Flow Filtration Show Higher Yield and Improved Activity. *Mol Ther* **26**, 2838-2847, doi:10.1016/j.ymthe.2018.09.015 (2018).

75 Rafiq, Q. A., Coopman, K., Nienow, A. W. & Hewitt, C. J. Systematic microcarrier screening and agitated culture conditions improves human

mesenchymal stem cell yield in bioreactors. *Biotechnol J* **11**, 473-486, doi:10.1002/biot.201400862 (2016).

76 Loubiere, C. *et al.* Impact of the type of microcarrier and agitation modes on the expansion performances of mesenchymal stem cells derived from umbilical cord. *Biotechnol Prog* **35**, e2887, doi:10.1002/btpr.2887 (2019).

77 Timmins, N. E. *et al.* Closed system isolation and scalable expansion of human placental mesenchymal stem cells. *Biotechnology and bioengineering* **109**, 1817-1826, doi:10.1002/bit.24425 (2012).

78 Yuan, Y., Kallos, M. S., Hunter, C. & Sen, A. Improved expansion of human bone marrow-derived mesenchymal stem cells in microcarrier-based suspension culture. *Journal of tissue engineering and regenerative medicine* **8**, 210-225, doi:10.1002/term.1515 (2014).

79 Nichol, J. W. *et al.* Cell-laden microengineered gelatin methacrylate hydrogels. *Biomaterials* **31**, 5536-5544, doi:10.1016/j.biomaterials.2010.03.064 (2010).

80 Hai, B., Shigemoto-Kuroda, T., Zhao, Q., Lee, R. H. & Liu, F. Inhibitory Effects of iPSC-MSCs and Their Extracellular Vesicles on the Onset of Sialadenitis in a Mouse Model of Sjogren's Syndrome. *Stem Cells Int* **2018**, 2092315, doi:10.1155/2018/2092315 (2018).

81 Nienow, A. W. *et al.* Agitation conditions for the culture and detachment of hMSCs from microcarriers in multiple bioreactor platforms. *Biochemical Engineering Journal* **108**, 24-29, doi:10.1016/j.bej.2015.08.003 (2016).

82 Leber, J. *et al.* Microcarrier choice and bead-to-bead transfer for human mesenchymal stem cells in serum-containing and chemically defined media. *Process Biochemistry* **59**, 255-265, doi:10.1016/j.procbio.2017.03.017 (2017).

83 Loessner, D. *et al.* Functionalization, preparation and use of cell-laden gelatin methacryloyl-based hydrogels as modular tissue culture platforms. *Nat Protoc* **11**, 727-746, doi:10.1038/nprot.2016.037 (2016).

84 Fairbanks, B. D., Schwartz, M. P., Bowman, C. N. & Anseth, K. S. Photoinitiated polymerization of PEG-diacrylate with lithium phenyl-2,4,6-trimethylbenzoylphosphinate: polymerization rate and cytocompatibility. *Biomaterials* **30**, 6702-6707, doi:10.1016/j.biomaterials.2009.08.055 (2009).

85 Sears, C. M. *Cell-derived matrices for bone tissue engineering*, Texas A&M University, (2019).

86 Yuan, X., Tsai, A. C., Farrance, I., Rowley, J. & Ma, T. Aggregation of Culture Expanded Human Mesenchymal Stem Cells in Microcarrier-based Bioreactor. *Biochem Eng J* **131**, 39-46, doi:10.1016/j.bej.2017.12.011 (2018).

87 Gregory, C. A. & Prockop, D. J. in *Culture of Human Stem Cells* 207-232 (2007).

88 Dos Santos, F. *et al.* Ex vivo expansion of human mesenchymal stem cells: a more effective cell proliferation kinetics and metabolism under hypoxia. *J Cell Physiol* **223**, 27-35, doi:10.1002/jcp.21987 (2010).

89 Krause, U., Seckinger, A. & Gregory, C. A. Assays of osteogenic differentiation by cultured human mesenchymal stem cells. *Methods Mol Biol* **698**, 215-230, doi:10.1007/978-1-60761-999-4_17 (2011).

90 Gregory, C. A. *et al.* Dkk-1-derived synthetic peptides and lithium chloride for the control and recovery of adult stem cells from bone marrow. *J Biol Chem* **280**, 2309-2323, doi:10.1074/jbc.M406275200 (2005).

91 Kim, D. K. *et al.* Chromatographically isolated CD63+CD81+ extracellular vesicles from mesenchymal stromal cells rescue cognitive impairments after TBI. *Proc Natl Acad Sci U S A* **113**, 170-175, doi:10.1073/pnas.1522297113 (2016).

92 Shigemoto-Kuroda, T. *et al.* MSC-derived Extracellular Vesicles Attenuate Immune Responses in Two Autoimmune Murine Models: Type 1 Diabetes and Uveoretinitis. *Stem Cell Reports* **8**, 1214-1225, doi:10.1016/j.stemcr.2017.04.008 (2017).

93 Amstad, E. *et al.* Robust scalable high throughput production of monodisperse drops. *Lab Chip* **16**, 4163-4172, doi:10.1039/c6lc01075j (2016).

94 Lee, B. H., Lum, N., Seow, L. Y., Lim, P. Q. & Tan, L. P. Synthesis and Characterization of Types A and B Gelatin Methacryloyl for Bioink Applications. *Materials (Basel, Switzerland)* **9**, doi:10.3390/ma9100797 (2016).

95 Rogers, R. E. *et al.* A scalable system for generation of mesenchymal stem cells derived from induced pluripotent cells employing bioreactors and degradable microcarriers. *Stem Cells Transl Med* **10**, 1650-1665, doi:10.1002/sctm.21-0151 (2021).

96 de Rutte, J. M., Koh, J. & Di Carlo, D. Scalable High-Throughput Production of Modular Microgels for In Situ Assembly of Microporous Tissue Scaffolds. *Advanced Functional Materials* **29**, 1900071, doi:10.1002/adfm.201900071 (2019).

97 Croughan, M. S., Sayre, E. S. & Wang, D. I. Viscous reduction of turbulent damage in animal cell culture. *Biotechnology and bioengineering* **33**, 862-872, doi:10.1002/bit.260330710 (1989).

98 Zhao, F., Chella, R. & Ma, T. Effects of shear stress on 3-D human mesenchymal stem cell construct development in a perfusion bioreactor system: Experiments and hydrodynamic modeling. *Biotechnology and bioengineering* **96**, 584-595, doi:10.1002/bit.21184 (2007).

99 Sousa, M. F. *et al.* Production of oncolytic adenovirus and human mesenchymal stem cells in a single-use, Vertical-Wheel bioreactor system: Impact of bioreactor design on performance of microcarrier-based cell culture processes. *Biotechnol Prog* **31**, 1600-1612, doi:10.1002/btpr.2158 (2015).

100 Frith, J. E., Thomson, B. & Genever, P. G. Dynamic three-dimensional culture methods enhance mesenchymal stem cell properties and increase therapeutic potential. *Tissue Eng Part C Methods* **16**, 735-749, doi:10.1089/ten.TEC.2009.0432 (2010).

101 Croughan, M., Giroux, D., Fang, D. & Lee, B. in *Stem Cell Manufacturing* 105-139 (Elsevier, 2016).

102 Schwarz, R. P., Goodwin, T. J. & Wolf, D. A. Cell culture for three-dimensional modeling in rotating-wall vessels: an application of simulated microgravity. *Journal of tissue culture methods : Tissue Culture Association manual of cell, tissue, and organ culture procedures* **14**, 51-57, doi:10.1007/BF01404744 (1992).

103 Zhao, X. *et al.* Photocrosslinkable Gelatin Hydrogel for Epidermal Tissue Engineering. *Adv Healthc Mater* **5**, 108-118, doi:10.1002/adhm.201500005 (2016).

104 Kirsch, M. *et al.* Gelatin-Methacryloyl (GelMA) Formulated with Human Platelet Lysate Supports Mesenchymal Stem Cell Proliferation and Differentiation and Enhances the Hydrogel's Mechanical Properties. *Bioengineering (Basel)* **6**, doi:10.3390/bioengineering6030076 (2019).

105 Cunha, B. *et al.* Bioprocess integration for human mesenchymal stem cells: From up to downstream processing scale-up to cell proteome characterization. *J Biotechnol* **248**, 87-98, doi:10.1016/j.jbiotec.2017.01.014 (2017).

106 Santos, F. *et al.* Toward a clinical-grade expansion of mesenchymal stem cells from human sources: a microcarrier-based culture system under xeno-free conditions. *Tissue Eng Part C Methods* **17**, 1201-1210, doi:10.1089/ten.tec.2011.0255 (2011).

107 Eibes, G. *et al.* Maximizing the ex vivo expansion of human mesenchymal stem cells using a microcarrier-based stirred culture system. *J Biotechnol* **146**, 194-197, doi:10.1016/j.jbiotec.2010.02.015 (2010).

108 Heathman, T. R. J. *et al.* Agitation and aeration of stirred-bioreactors for the microcarrier culture of human mesenchymal stem cells and potential implications for large-scale bioprocess development. *Biochemical Engineering Journal* **136**, 9-17, doi:10.1016/j.bej.2018.04.011 (2018).

109 Vater, C., Kasten, P. & Stiehler, M. Culture media for the differentiation of mesenchymal stromal cells. *Acta Biomater* **7**, 463-477, doi:10.1016/j.actbio.2010.07.037 (2011).

110 Prockop, D. J., Oh, J. Y. & Lee, R. H. Data against a Common Assumption: Xenogeneic Mouse Models Can Be Used to Assay Suppression of Immunity by Human MSCs. *Mol Ther* **25**, 1748-1756, doi:10.1016/j.ymthe.2017.06.004 (2017).

111 Guerrouahen, B. S., Sidahmed, H., Al Sulaiti, A., Al Khulaifi, M. & Cugno, C. Enhancing Mesenchymal Stromal Cell Immunomodulation for Treating Conditions Influenced by the Immune System. *Stem Cells Int* **2019**, 7219297, doi:10.1155/2019/7219297 (2019).

112 Mendicino, M., Bailey, A. M., Wonnacott, K., Puri, R. K. & Bauer, S. R. MSC-based product characterization for clinical trials: an FDA perspective. *Cell Stem Cell* **14**, 141-145, doi:10.1016/j.stem.2014.01.013 (2014).

113 McGrath, M. *et al.* GMP-compatible and xeno-free cultivation of mesenchymal progenitors derived from human-induced pluripotent stem cells. *Stem Cell Res Ther* **10**, 11, doi:10.1186/s13287-018-1119-3 (2019).

114 Sondergaard, R. H. *et al.* Senescence and quiescence in adipose-derived stromal cells: Effects of human platelet lysate, fetal bovine serum and hypoxia. *Cytotherapy* **19**, 95-106, doi:10.1016/j.jcyt.2016.09.006 (2017).

115 Abdelrazik, H., Spaggiari, G. M., Chiossone, L. & Moretta, L. Mesenchymal stem cells expanded in human platelet lysate display a decreased inhibitory capacity on T- and NK-cell proliferation and function. *Eur J Immunol* **41**, 3281-3290, doi:10.1002/eji.201141542 (2011).

116 Flemming, A. *et al.* Immunomodulative efficacy of bone marrow-derived mesenchymal stem cells cultured in human platelet lysate. *J Clin Immunol* **31**, 1143-1156, doi:10.1007/s10875-011-9581-z (2011).

117 Ben Azouna, N. *et al.* Phenotypical and functional characteristics of mesenchymal stem cells from bone marrow: comparison of culture using different media supplemented with human platelet lysate or fetal bovine serum. *Stem Cell Res Ther* **3**, 6, doi:10.1186/scrt97 (2012).

118 Oikonomopoulos, A. *et al.* Optimization of human mesenchymal stem cell manufacturing: the effects of animal/xeno-free media. *Sci Rep* **5**, 16570, doi:10.1038/srep16570 (2015).

119 Gao, F. *et al.* Mesenchymal stem cells and immunomodulation: current status and future prospects. *Cell Death Dis* **7**, e2062, doi:10.1038/cddis.2015.327 (2016).

120 Pachler, K. *et al.* A Good Manufacturing Practice-grade standard protocol for exclusively human mesenchymal stromal cell-derived extracellular vesicles. *Cytotherapy* **19**, 458-472, doi:10.1016/j.jcyt.2017.01.001 (2017).

121 Mojica-Henshaw, M. P. *et al.* Serum-converted platelet lysate can substitute for fetal bovine serum in human mesenchymal stromal cell cultures. *Cytotherapy* **15**, 1458-1468, doi:10.1016/j.jcyt.2013.06.014 (2013).

122 Lee, R. H. *et al.* TSG-6 as a biomarker to predict efficacy of human mesenchymal stem/progenitor cells (hMSCs) in modulating sterile inflammation in vivo. *Proc Natl Acad Sci U S A* **111**, 16766-16771, doi:10.1073/pnas.1416121111 (2014).

123 McNeill, E. P. *et al.* Characterization of a pluripotent stem cell-derived matrix with powerful osteoregenerative capabilities. *Nat Commun* **11**, 3025, doi:10.1038/s41467-020-16646-2 (2020).

124 Marklein, R. A. *et al.* Morphological profiling using machine learning reveals emergent subpopulations of interferon-gamma-stimulated mesenchymal stromal cells that predict immunosuppression. *Cytotherapy* **21**, 17-31, doi:10.1016/j.jcyt.2018.10.008 (2019).

125 Laner-Plamberger, S. *et al.* Upregulation of mitotic bookmarking factors during enhanced proliferation of human stromal cells in human platelet lysate. *J Transl Med* **17**, 432, doi:10.1186/s12967-019-02183-0 (2019).

126 Chang, Y. L., Stanford, C. M. & Keller, J. C. Calcium and phosphate supplementation promotes bone cell mineralization: implications for hydroxyapatite (HA)-enhanced bone formation. *J Biomed Mater Res* **52**, 270-278, doi:10.1002/1097-4636(200011)52:2<270::aid-jbm5>3.0.co;2-1 (2000).

127 Lin, Y. M. *et al.* Expansion in microcarrier-spinner cultures improves the chondrogenic potential of human early mesenchymal stromal cells. *Cytotherapy* **18**, 740-753, doi:10.1016/j.jcyt.2016.03.293 (2016).

128 Bernardo, M. E. *et al.* Optimization of in vitro expansion of human multipotent mesenchymal stromal cells for cell-therapy approaches: further insights in the search for a fetal calf serum substitute. *J Cell Physiol* **211**, 121-130, doi:10.1002/jcp.20911 (2007).

129 Castegnaro, S. *et al.* Effect of platelet lysate on the functional and molecular characteristics of mesenchymal stem cells isolated from adipose tissue. *Curr Stem Cell Res Ther* **6**, 105-114, doi:10.2174/157488811795495440 (2011).

APPENDIX A

Table 2: List of Primer Sequences Used in This Study

Target	Sequence
GAPDH	FOR CTCTCTGCTCCTCCTGTTCGAC REV TGAGCGATGTGGCTCGGCT
collagen I	FOR GAACGCGTGTCATCCCTTGT REV GAACGAGGTAGTCTTTCAGCAACA
runx2	FOR GCAAGGTTCAACGATCTGAGA REV TCCCCGAGGTCCATCTACTG
alkaline phosphatase	FOR GACCCTTGACCCCCACAAT REV GCTCGTACTGCATGTCCCCT
osteocalcin	FOR TGAGAGCCCTCACACTCC REV CGCCTGGGTCTCTTCACTAC
PPAR gamma	FOR CACAAGAACAGATCCAGTGGTTGCAG REV AATAATAAGGTGGAGATGCAGGCTCC
FABP4	FOR TCAGTGTGAATGGGGATGTGA REV TCAACGTCCCTTGGCTTATGC
lipoprotein lipase	FOR GGAATGTATGAGAGTTGGGT REV GGGCTTCTGCATACTCAAAG